Chapter 3
Classical and First-Order Shear Deformation Analysis of Sandwich Plates

This chapter will present classical laminated plate theory (CLPT) analysis of composite face sheets and sandwich plates. It is recognized that the transverse shear deformation is not incorporated in CLPT. Shear deformation of sandwich plates is important and first-order shear deformation analysis will be outlined. Applications of CLPT and first-order shear deformation analysis to sandwich panels will be presented. Two experimental sandwich plate tests, viz. bending under transverse pressure load and twisting, will be described. Experimental data generated from such tests will be compared to predictions from plate theory analysis and finite elements.

3.1 Classical Laminated Plate Theory Analysis

Classical laminated plate theory (CLPT) aims to relate the mechanical response of a layered plate to that of the individual constituent piles. This theory is an extension of the theory for homogeneous isotropic plates presented by Timoshenko and Woinowsky-Krieger (1959) to thin laminated plates. The analysis is most appropriate for thin plates since, as will be shown, this theory does not accommodate transverse shear deformation. Hence, CLPT is of limited applicability to sandwich panels since they often possess a thick, shear deformable core. CLPT, however, is applicable to the analysis of the in-plane response of face sheets and, furthermore, constitutes an important reference for sandwich panels with in-plane dimensions much greater than the thickness.

L.A. Carlsson and G.A. Kardomateas, *Structural and Failure Mechanics of Sandwich Composites*, Solid Mechanics and its Applications 121, DOI 10.1007/978-1-4020-3225-7_3,

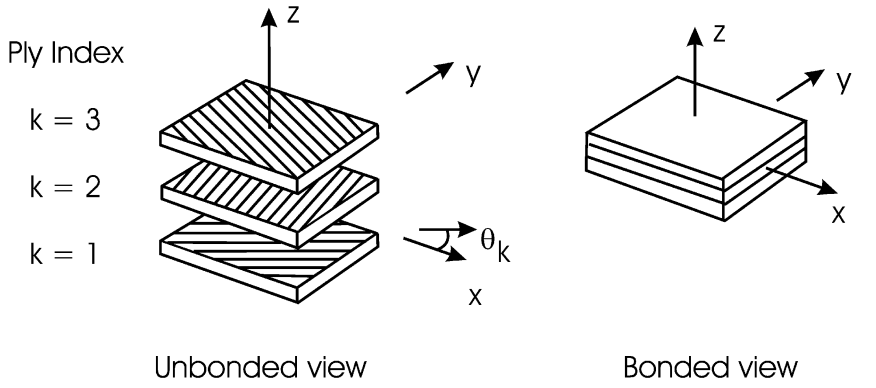

Figure 3.1 Unbonded and bonded views of a multi-ply laminate consisting of N plies.

3.1.1 Laminate Nomenclature

Figure 3.1 shows unbonded and bonded views of a laminate consisting of N orthotropic plies with the fibers oriented at any in-plane direction, θ.

The plies may be unidirectional (as shown) or fabric weaves. For fabric weaves, the angle θ refers to the warp or weft fiber directions. Figure 3.1 also illustrates the global xyz laminate coordinate system and the local (ply) coordinate system 123, where the 3 axis is parallel to the thickness coordinate (z) of the laminated plate. The plies in the laminate are numbered $1, 2, \ldots, N$ from bottom and up. The ply index, k, identifies the particular ply considered, and θ_k denotes the orientation of ply k.

For the purpose of subsequent analysis, the "ply coordinates", z_k, are defined in Figure 3.2. The origin of the z coordinate is located at the mid-plane of the laminate. Hence, $z_0 = -h/2$ and $z_N = h/2$, where h is the total thickness of the laminate (Figure 3.2). The ply coordinates indicate the location of the ply interfaces, and ply k is bound by z_{k-1} and z_k.

The lay-up sequence of a laminate is standardized, see Adams et al. (2003). The ply orientations in degrees are listed within brackets starting with the first ply laid up, followed by a slash (/) and then the next ply, and so on until the top ply. For symmetric laminates, only the bottom half of the plies are shown, and a subscript capital S follows the right closing bracket. For example, a six-ply symmetric laminate with plies oriented at 45°, 0°, −30°, −30°, 0° and 45° would be expressed as $[45/0/-30]_s$. For symmet-

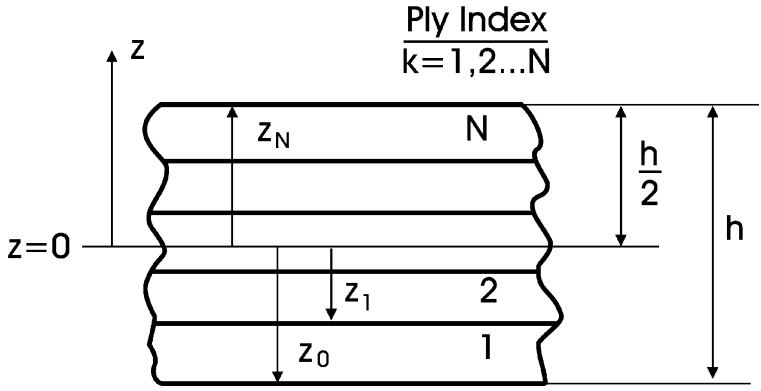

Figure 3.2 Definition of the ply coordinates, z_k.

ric laminates with an odd number of plies, the center ply is designated with an overbar.

3.1.2 Kinematics of Deformation

Figure 3.3 shows a flat composite laminate plate before loading and the xyz coordinate system. Deformation of the laminate plate is expressed using the displacement vector

$$\mathbf{u} = u\mathbf{i} + v\mathbf{j} + w\mathbf{k}, \tag{3.1}$$

where (u, v, w) are the components of the displacement vector (Figure 3.3) and $\mathbf{i}, \mathbf{j}, \mathbf{k}$ are the unit vectors for the x, y, z coordinates. From the displacement components, we can determine the extensional and shear strains,

$$\varepsilon_x = \frac{\partial u}{\partial x}, \tag{3.2a}$$

$$\varepsilon_y = \frac{\partial v}{\partial y}, \tag{3.2b}$$

$$\varepsilon_z = \frac{\partial w}{\partial z}, \tag{3.2c}$$

$$\gamma_{yz} = \frac{\partial v}{\partial z} + \frac{\partial w}{\partial y}, \tag{3.2d}$$

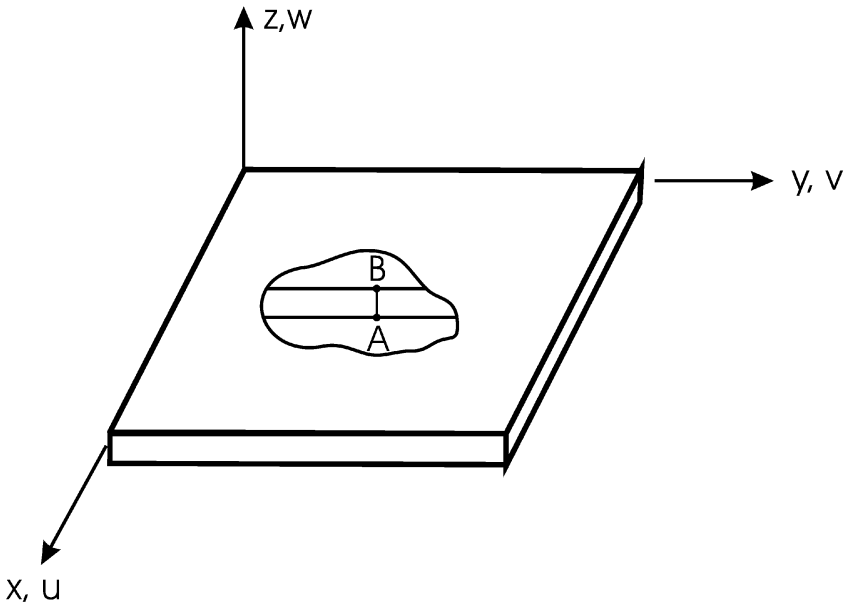

Figure 3.3 Composite laminate plate before deformation and definition of displacement components.

$$y_{xz} = \frac{\partial u}{\partial z} + \frac{\partial w}{\partial x}, \tag{3.2e}$$

$$y_{xy} = \frac{\partial u}{\partial y} + \frac{\partial v}{\partial x}. \tag{3.2f}$$

Notice here that the strains are assumed to be small ($\ll 1$), since Equations (3.2) include only first-order derivatives.

Figure 3.3 shows an element of the interior of the laminated plate cut parallel to the y axis. The deformation of this element will be examined in detail. Figure 3.4 illustrates the element before and after deformation.

When the laminate plate is loaded, the cross-section defined by the line AB, originally straight and perpendicular to the reference plane ($z = 0$) will translate and rotate as shown in Figure 3.4. The y and z axis displacements of the point O, on the mid-plane, are v_0 and w_0 (Figure 3.4). It is assumed that the line segment AB remains straight and normal to the deformed mid-plane. Further, the segment is assumed to maintain its length during deformation, implying

$$w(x, y) = w_0(x, y), \tag{3.3}$$

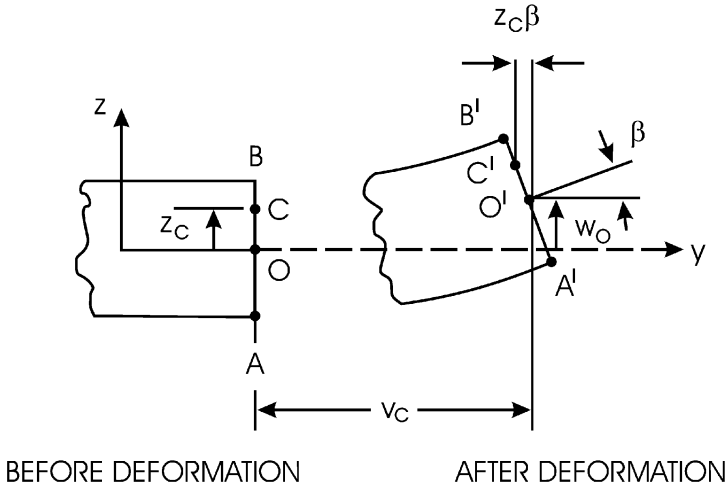

Figure 3.4 Element of plate cut parallel to the x axis before and after deformation.

where subscript zero refers to the mid-plane ($z = 0$). The assumptions constitutes the famous Kirchhoff hypothesis for plates, and implies that flat sections originally oriented normal to the mid-plane remain flat and normal to the deformed mid-plane after loading.

Further, because the line AB remains straight and perpendicular to the deformed mid-plane, the slope of the cross-section, β, in Figure 3.4, is equal to the slope of the panel, i.e.,

$$\beta = \frac{\partial w_0}{\partial y}. \tag{3.4}$$

The y axis displacement of point C, at a distance z_c from the mid-plane, becomes

$$v_c = v_0 - \beta z_c. \tag{3.5}$$

For any point on the line segment we will get

$$v = v_0 - \beta z. \tag{3.6}$$

Substitution of Equation (3.4) into (3.6) yields

$$v(x, y, z) = v_0(x, y) - z\frac{\partial w_0}{\partial y}. \tag{3.7}$$

Consideration of a cross-section of the plate cut parallel to the x axis similarly yields

$$u(x, y, z) = u_0(x, y) - z\frac{\partial w_0}{\partial x}. \tag{3.8}$$

Equations (3.3), (3.7) and (3.8) provide the necessary expressions for the displacements of the laminate plate. Differentiation of these expressions, according to Equations (3.2), yields

$$\varepsilon_x = \frac{\partial u_0}{\partial x} - z\frac{\partial^2 w_0}{\partial x^2}, \tag{3.9a}$$

$$\varepsilon_y = \frac{\partial v_0}{\partial y} - z\frac{\partial^2 w_0}{\partial y^2}, \tag{3.9b}$$

$$\varepsilon_z = 0, \tag{3.9c}$$

$$\gamma_{yz} = 0 = \gamma_{xz}, \tag{3.9d}$$

$$\gamma_{xy} = \frac{\partial u_0}{\partial y} + \frac{\partial v_0}{\partial x} - 2z\frac{\partial^2 w_0}{\partial x \partial y}. \tag{3.9e}$$

Hence, the CLPT does not accommodate transverse shear deformation and thickness stretch. The only non-zero strains are the in-plane strains $\varepsilon_x, \varepsilon_y$ and γ_{xy}. These strains are commonly expressed in the following form

$$\begin{bmatrix} \varepsilon_x \\ \varepsilon_y \\ \gamma_{xy} \end{bmatrix} = \begin{bmatrix} \varepsilon_x^0 \\ \varepsilon_y^0 \\ \gamma_{xy}^0 \end{bmatrix} + z \begin{bmatrix} \kappa_x \\ \kappa_y \\ \kappa_{xy} \end{bmatrix}, \tag{3.10}$$

where $[\varepsilon_x^0, \varepsilon_y^0, \gamma_{xy}^0]$ and $[\kappa_x, \kappa_y, \kappa_{xy}]$ are the strains and curvatures of the reference mid-plane, defined according to Equations (3.9) as

$$\varepsilon_x^0 = \frac{\partial u_0}{\partial x}, \tag{3.11a}$$

$$\varepsilon_y^0 = \frac{\partial v_0}{\partial y}, \tag{3.11b}$$

$$\gamma_{xy}^0 = \frac{\partial u_0}{\partial y} + \frac{\partial v_0}{\partial x}, \tag{3.11c}$$

$$\kappa_x = -\frac{\partial^2 w_0}{\partial x^2}, \tag{3.12a}$$

$$\kappa_y = -\frac{\partial^2 w_0}{\partial y^2}, \tag{3.12b}$$

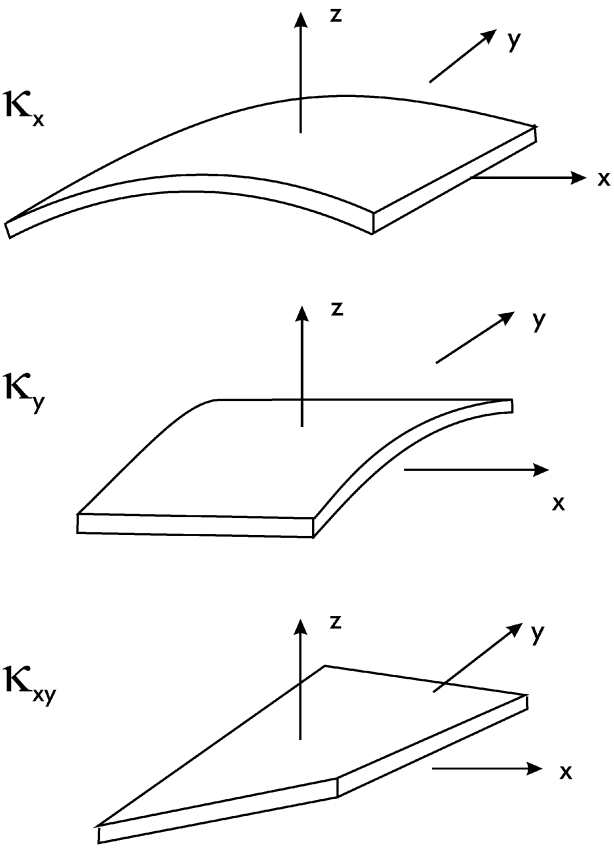

Figure 3.5 Illustration of bending and twisting deformation of a laminated plate. All curvatures shown are positive.

$$\kappa_{xy} = -2\frac{\partial^2 w_0}{\partial x \partial y}. \tag{3.12c}$$

The mid-plane strains signify membrane loading, since they represent extension and shear deformation of the mid-plane. The curvatures, κ_x and κ_y, represent bending deformation, while the curvature, κ_{xy}, represents twisting of the laminated plate, see Figure 3.5.

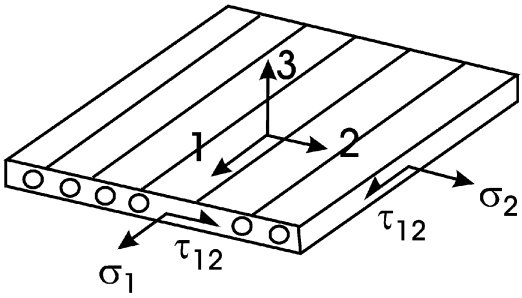

Figure 3.6 Orthotropic ply under in-plane stresses σ_1, σ_2 and τ_{12}.

3.1.3 Stresses in the Laminate

Consider a thin orthotropic ply with the principal material directions 1-2-3 loaded in the 1-2 plane of the ply as shown in Figure 3.6. The relation between stresses $[\sigma_1, \sigma_2, \tau_{12}]$ and strains $[\varepsilon_1, \varepsilon_2, \gamma_{12}]$ becomes (Hyer, 1998)

$$\begin{bmatrix} \sigma_1 \\ \sigma_2 \\ \tau_{12} \end{bmatrix} = \begin{bmatrix} Q_{11} & Q_{12} & 0 \\ Q_{12} & Q_{22} & 0 \\ 0 & 0 & Q_{66} \end{bmatrix} \begin{bmatrix} \varepsilon_1 \\ \varepsilon_2 \\ \gamma_{12} \end{bmatrix}, \tag{3.13}$$

where the stiffness, Q_{ij}, can be expressed

$$Q_{11} = E_1/(1 - \nu_{112}\nu_{21}), \tag{3.14a}$$

$$Q_{12} = \nu_{12}E_2/(1 - \nu_{12}\nu_{21}) = \nu_{21}E_1/(1 - \nu_{12}\nu_{21}), \tag{3.14b}$$

$$Q_{22} = E_2/(1 - \nu_{12}\nu_{21}), \tag{3.14c}$$

$$Q_{66} = G_{12}. \tag{3.14d}$$

Here, E_1 and E_2 represent the principal moduli in the fiber direction (1 in Figure 3.6) and the transverse direction (2 in Figure 3.6). ν_{12} and ν_{21} are the associated Poisson ratios, and G_{12} is the in-plane shear modulus.

For a ply within the laminate where the fibers are oriented at an angle, θ, to the global x coordinate of the laminate, Figure 3.7, the stresses, strains, and stiffnesses must be transformed to the new x–y axes. It may be shown that transformed relation between in-plane stresses and strains for the "off-axis" ply, Figure 3.7, will take the following form (Hyer, 1998):

$$\begin{bmatrix} \sigma_x \\ \sigma_y \\ \tau_{xy} \end{bmatrix}_k = \begin{bmatrix} \bar{Q}_{11}\bar{Q}_{12}\bar{Q}_{16} \\ \bar{Q}_{12}\bar{Q}_{22}\bar{Q}_{26} \\ \bar{Q}_{16}\bar{Q}_{26}\bar{Q}_{66} \end{bmatrix}_k \begin{bmatrix} \varepsilon_x \\ \varepsilon_y \\ \gamma_{xy} \end{bmatrix}, \tag{3.15}$$

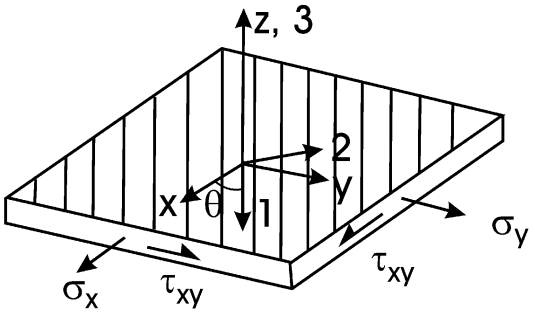

Figure 3.7 Off-axis ply element under in-plane loading.

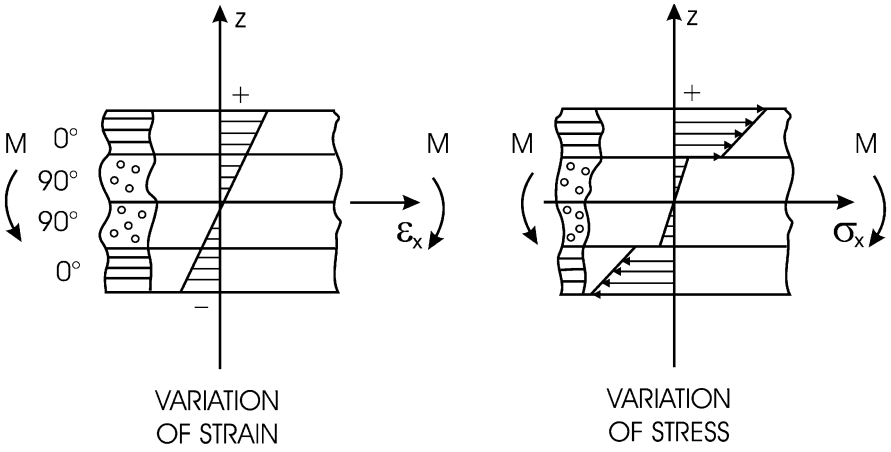

Figure 3.8 Variations of bending strain and stress in a $[0/90]_s$ laminate subject to pure bending loading.

where the elements, $\bar{Q}_{ij}$, of the stiffness matrix for ply k are defined in terms of the principal stiffnesses, Q_{ij}, and the ply orientation, θ_k, in Appendix A. The subscript k on the stresses signifies that the stresses may vary in a discontinuous manner from ply to ply, even if the strains vary in a continuous manner (Equations (3.10)).

Figure 3.8 illustrates the variations of strain, ε_x, and stress, σ_x, in a $[0/90]_s$ laminate under pure bending load. The stress, σ_x, is greater in the 0° plies than the 90° plies because the 0° plies have the fibers aligned with the longitudinal direction (x axis), while the 90° plies have the fibers aligned with the y axis. Typically, Young's modulus (E) is a factor 5–15 greater in the 0° direction than in the transverse direction.

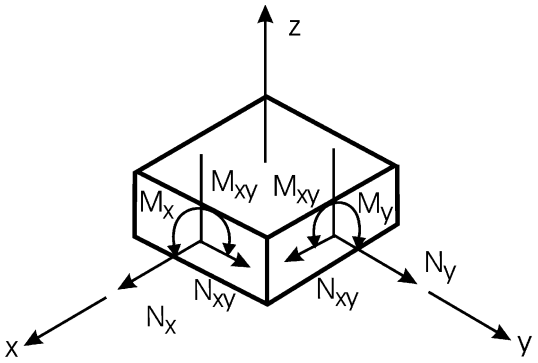

Figure 3.9 Force and moment resultants for an element of a laminate plate.

3.1.4 Force and Moment Resultants

Force and moment resultants, defined for an element of the laminate (Figure 3.9), are obtained by integrating the stresses over the thickness of the laminate

$$(N_x, N_y, N_{xy}) = \int_{-h/2}^{h/2} (\sigma_x, \sigma_y, \tau_{xy}) dz, \tag{3.16a}$$

$$(M_x, M_y, M_{xy}) = \int_{-h/2}^{h/2} (\sigma_x, \sigma_y, \tau_{xy}) z dz. \tag{3.16b}$$

Because the stresses vary in a continuous manner within a ply but may jump across the ply boundaries as shown in Figure 3.8, the integrations are conducted for each ply (k) defined by the ply coordinates z_{k-1} and z_k, and then the results are added.

$$\begin{bmatrix} N_x \\ N_y \\ N_{xy} \end{bmatrix} = \int_{-h/2}^{h/2} \begin{bmatrix} \sigma_x \\ \sigma_y \\ \tau_{xy} \end{bmatrix} dz = \sum_{k=1}^{N} \int_{z_{k-1}}^{z_k} \begin{bmatrix} \sigma_x \\ \sigma_y \\ \tau_{xy} \end{bmatrix}_k dz, \tag{3.17a}$$

$$\begin{bmatrix} M_x \\ M_y \\ M_{xy} \end{bmatrix} = \int_{-h/2}^{h/2} \begin{bmatrix} \sigma_x \\ \sigma_y \\ \tau_{xy} \end{bmatrix} z dz = \sum_{k=1}^{N} \int_{z_{k-1}}^{z_k} \begin{bmatrix} \sigma_x \\ \sigma_y \\ \tau_{xy} \end{bmatrix}_k z dz. \tag{3.17b}$$

The force and moment resultants have units of force per unit length and moment per unit length, and are generally dependent on the in-plane coordinates, x and y, but do not depend on the thickness coordinate (z) after integration.

Substitution of the in-plane stresses given by Equations (3.15) into (3.17) yields, after integration,

$$\begin{bmatrix} N_x \\ N_y \\ N_{xy} \end{bmatrix} = \begin{bmatrix} A_{11}A_{12}A_{16} \\ A_{12}A_{22}A_{26} \\ A_{16}A_{26}A_{66} \end{bmatrix} \begin{bmatrix} \varepsilon_x^0 \\ \varepsilon_y^0 \\ \gamma_{xy}^0 \end{bmatrix} + \begin{bmatrix} B_{11}B_{12}B_{16} \\ B_{12}B_{22}B_{26} \\ B_{16}B_{26}B_{66} \end{bmatrix} \begin{bmatrix} \kappa_x \\ \kappa_y \\ \kappa_{xy} \end{bmatrix}, \tag{3.18}$$

$$\begin{bmatrix} M_x \\ M_y \\ M_{xy} \end{bmatrix} = \begin{bmatrix} B_{11}B_{12}B_{16} \\ B_{12}B_{22}B_{26} \\ B_{16}B_{26}B_{66} \end{bmatrix} \begin{bmatrix} \varepsilon_y^0 \\ \varepsilon_y^0 \\ \gamma_{xy}^0 \end{bmatrix} + \begin{bmatrix} D_{11}D_{12}D_{16} \\ D_{12}D_{22}D_{26} \\ D_{16}D_{26}D_{66} \end{bmatrix} \begin{bmatrix} \kappa_x \\ \kappa_y \\ \kappa_{xy} \end{bmatrix}. \tag{3.19}$$

The $[A]$, $[B]$, and $[D]$ matrices in Equations (3.18) and (3.19) govern the response of a laminated plate to forces and moments. The $[A]$ matrix is called "extensional stiffness matrix", the $[B]$ matrix is called "coupling stiffness matrix", and the $[D]$ matrix is called "bending stiffness matrix" in accordance with their roles for the mechanical behavior of a laminated plate. The $[A]$ matrix relates extensional and shear strains to the force resultants, and the $[D]$ matrix relates bending and twisting curvatures to the moment resultants. The $[B]$ matrix appears both in the equations for the force resultants and moment resultants and acts to couple the responses in extension and bending.

The elements of the stiffness matrices are given by

$$A_{ij} = \sum_{k=1}^{N} (\bar{Q}_{ij})_k (z_k - z_{k-1}), \tag{3.20a}$$

$$B_{ij} = \frac{1}{2} \sum_{k=1}^{N} (\bar{Q}_{ij})_k (z_k^2 - z_{k-1}^2), \tag{3.20b}$$

$$D_{ij} = \frac{1}{3} \sum_{k=1}^{N} (\bar{Q}_{ij})_k (z_k^3 - z_{k-1}^3). \tag{3.20c}$$

It may be shown that $B_{ij} = 0$ in Equations (3.18) and (3.19) for laminates with a symmetrical lay-up sequence. Hence, such laminates possess no coupling between the extensional and bending responses which greatly simplifies the analysis of the response. Face laminates are commonly laid-up in a symmetric manner. Furthermore, face laminates are usually "balanced", which means that for an off-axis ply with fiber orientation angle θ, there is a corresponding layer with orientation angle $-\theta$, which will have the consequence that $A_{16} = A_{26} = 0$ in Equations (3.18). These terms, if non-zero, signify coupling between extensional and shear response, which is undesirable.

3.1.5 Effective Engineering Elastic Constants of Laminates

When analyzing sandwich beams and panels, it is convenient to establish the effective engineering constants of the face laminates. Such constants are primarily the in-plane extensional and shear moduli, although sometimes the out-of-plane moduli are demanded. In this section we will present method to calculate the in-plane engineering constants based on the laminate extensional stiffness matrix.

Consider a symmetric and balanced laminated plate. According to the discussion in Section 3.1.4, the response to in-plane loading is given by

$$\begin{bmatrix} N_x \\ N_y \\ N_{xy} \end{bmatrix} = \begin{bmatrix} A_{11} & A_{12} & 0 \\ A_{12} & A_{22} & 0 \\ 0 & 0 & A_{66} \end{bmatrix} \begin{bmatrix} \varepsilon_x \\ \varepsilon_y \\ \gamma_{xy} \end{bmatrix}. \tag{3.21}$$

Notice here that the laminate strains coincide with the mid-plane strains due to the absence of bending curvatures (Equations (3.10)). For the purpose of establishing the effective engineering constants, it is more convenient to use the compliance (inverted) version of Equation (3.21), i.e.,

$$\begin{bmatrix} \varepsilon_x \\ \varepsilon_y \\ \gamma_{xy} \end{bmatrix} = \begin{bmatrix} a_{11} & a_{12} & 0 \\ a_{12} & a_{22} & 0 \\ 0 & 0 & a_{66} \end{bmatrix} \begin{bmatrix} N_x \\ N_y \\ N_{xy} \end{bmatrix}, \tag{3.22}$$

where

$$a_{11} = \frac{A_{22}}{A_{11}A_{22} - A_{12}^2}, \tag{3.23a}$$

$$a_{12} = \frac{-A_{12}}{A_{11}A_{22} - A_{12}^2}, \tag{3.23b}$$

$$a_{22} = \frac{A_{11}}{A_{11}A_{22} - A_{12}^2}, \tag{3.23c}$$

$$a_{66} = \frac{1}{A_{66}}. \tag{3.23d}$$

To further facilitate the deformation of the engineering constants, it is recognized that the average stresses $\bar{\sigma}_x$, $\bar{\sigma}_y$ and $\bar{\tau}_{xy}$ are given by

$$\bar{\sigma}_x = \frac{N_x}{h}, \tag{3.24a}$$

$$\bar{\sigma}_y = \frac{N_y}{h}, \tag{3.24b}$$

$$\bar{\tau}_{xy} = \frac{N_{xy}}{h}. \tag{3.24c}$$

With this, Equations (3.22) may be written as

$$\begin{bmatrix} \varepsilon_x \\ \varepsilon_y \\ \gamma_{xy} \end{bmatrix} = h \begin{bmatrix} a_{11} & a_{12} & 0 \\ a_{12} & a_{22} & 0 \\ 0 & 0 & a_{66} \end{bmatrix} \begin{bmatrix} \bar{\sigma}_x \\ \bar{\sigma}_y \\ \bar{\gamma}_{xy} \end{bmatrix}. \tag{3.25}$$

These equations may be compared to those for an orthotropic homogeneous material loaded in the principal system (Figure 3.6)

$$\begin{bmatrix} \varepsilon_1 \\ \varepsilon_2 \\ \gamma_{12} \end{bmatrix} = \begin{bmatrix} l/E_1 & -\nu_{12}/E_1 & 0 \\ -\nu_{21}/E_2 & 1/E_2 & 0 \\ 0 & 0 & 1/G_{12} \end{bmatrix} \begin{bmatrix} \sigma_1 \\ \sigma_2 \\ \tau_{12} \end{bmatrix}. \tag{3.26}$$

Direct comparison between Equations (3.25) and (3.26) yields the effective engineering constants of the laminated plate according to

$$E_x = \frac{1}{ha_{11}}, \tag{3.27a}$$

$$\nu_{xy} = \frac{-a_{12}}{a_{11}}, \tag{3.27b}$$

$$E_y = \frac{1}{ha_{22}}, \tag{3.27c}$$

$$\nu_{yx} = \frac{-a_{12}}{a_{22}}, \tag{3.27d}$$

$$G_{xy} = \frac{1}{ha_{66}}. \tag{3.27e}$$

Notice also that the Poisson ratios are not independent

$$\nu_{xy} = \nu_{xy} \frac{E_x}{E_y}, \tag{3.28}$$

which conforms to established orthotropic material behavior.

Equations (3.27) are very convenient for reducing a large set of ply mechanical properties and ply orientation angles into a set of four independent engineering constants.

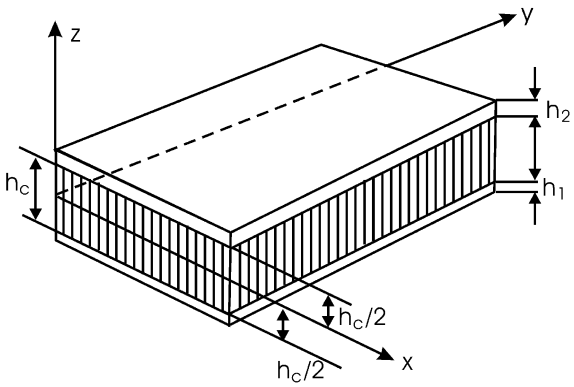

Figure 3.10 Definition of nomenclatures for sandwich plate.

For estimation of the effective out-of-plane stiffnesses E_z, G_{xz} and G_{yx} of the laminate several methods exists, see, e.g., Chou et al. (1972) and Bogetti et al. (2004). It should be pointed out that such methods are much more involved than the determination of the in-plane engineering constants. As a first estimate for a laminate consisting of transversely isotropic plies, it could be assumed that

$$E_z \cong E_3 = E_2, \tag{3.29a}$$

$$G_{xz} \cong G_{yz} \cong G_{13} = G_{12}. \tag{3.29b}$$

Such estimates are expected to be reasonable for laminates utilizing unidirectional transversely isotropic plies, where the properties in the out-of-plane direction should be close to those in the in-plane transverse direction.

3.2 First-Order Shear Deformation Analysis of a Sandwich Plate

Consider a sandwich plate consisting of face sheets of thicknesses h_1 and h_2, and a core of thickness h_c, see Figure 3.10. The faces and core may be isotropic or orthotropic with their principal directions along xyz, see Figure 3.10. The core may be corrugated (web), honeycomb, a foamed material, or balsa wood, (Figure 1.4). Such cores display macroscopic mechanical behavior that may be characterized as isotropic or orthotropic, i.e. having three mutually perpendicular planes of elastic symmetry (Hyer, 1998).

The early texts on sandwich structures forwarded by Plantema (1966) and Allen (1969), as well as the more recent text by Zenkert (1997), analyze the deflection, w, of sandwich panels using "partial deflections", i.e., deflections

due to bending and shear separately, and obtain the total deflection by adding solutions for each mode of deformation. Analysis of sandwich plates and beams, however, is most conveniently performed extending the first-order shear deformation theory for homogeneous and isotropic plates developed by Reissner (1945) and Mindlin (1951) to sandwich plates with orthotropic face sheets. Such extensions were done by several authors, e.g. Libove and Batdorf (1948) and Whitney (1987). In this text we will forward the first-order shear deformation plate theory in a form similar to that presented for flat sandwich panels by Whitney (1987) who assumed that the in-plane displacements u and v of the faces are those at the face/core interfaces. Here we will modify the Whitney theory by assuming that the in-plane displacements of the faces are those at the centroids of the face sheets. This is consistent with traditional sandwich theory (Allen, 1969).

Figure 3.10 shows that the origin of the coordinate system xyz is placed at the center of the core, i.e., $z = 0$ in the core mid-plane. This is different from classical laminated plate theory where $z = 0$ in the geometrical mid-plane of the panel (Figure 3.10). The analysis is based on the following assumptions:

(i) The face sheets are thin compared to the core, i.e., $h_1, h_2 \ll h_c$ and in a state of plane stress ($\sigma_z = \tau_{xz} = \tau_{yz} = 0$).
(ii) The in-plane stresses, σ_x, σ_y, and τ_{xy}, in the core are negligible.
(iii) In-plane displacements, u and v, are uniform through the thickness of the face sheets and assume their mid-plane (centroidal) values.
(iv) The out-of-plane displacement, w, is independent of the z coordinate, i.e., the thickness strain, $\varepsilon_z = \partial w/\partial z = 0$.
(v) The in-plane displacements in the core, u and v, are linear in the thickness coordinate, z.

Based on the assumptions (iv) and (v), the displacements of the core are

$$u = u_0(x, y) + z\psi_x(x, y), \tag{3.30a}$$

$$v = v_0(x, y) + z\psi_y(x, y), \tag{3.30b}$$

$$w = w_0(x, y), \tag{3.30c}$$

where u_0, v_0 and w_0 are the displacements at the core mid-plane, see Figure 3.11, and ψ_x and ψ_y are the rotations of cross-sections originally perpendicular to the x and y axes, respectively. From continuity of displacements at the face/core interfaces ($z = \pm h_c/2$), and assumption (iii), the displacements of the bottom and top face sheets become (Figure 3.11)

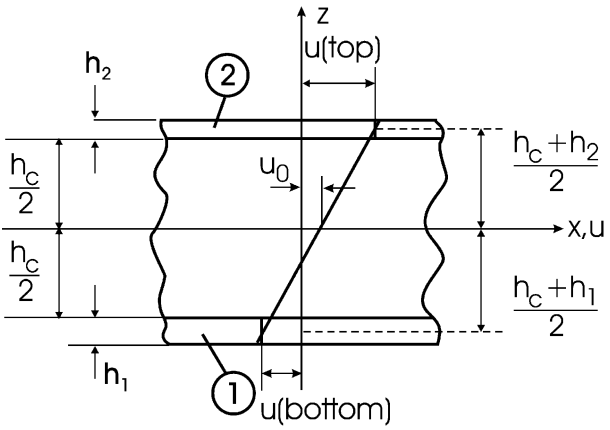

Figure 3.11 Illustration of displacement u for sandwich element oriented along the x axis.

$$u(\text{bottom}) = u_0 - \frac{(h_c + h_1)}{2}\psi_x, \tag{3.31a}$$

$$u(\text{top}) = u_0 + \frac{(h_c + h_2)}{2}\psi_x, \tag{3.31b}$$

$$v(\text{bottom}) = v_0 - \frac{(h_c + h_1)}{2}\psi_y, \tag{3.31c}$$

$$v(\text{top}) = v_0 + \frac{(h_c + h_2)}{2}\psi_y, \tag{3.31d}$$

$$w = w_0, \tag{3.31e}$$

where "bottom" and "top" refer to the lower and upper face sheets, respectively.

Figure 3.12 shows a section of a sandwich plate cut in the x–z plane. The core element ACFD represents a section of the core with the surfaces AC and DF perpendicular to the x axis before deformation. After deformation, point B displaces to assume a position at B′, and the vertical upwards displacement of point B (originally at $z = 0$) is w, and that of the adjacent point E assuming the new position E′ is $w + (\partial w/\partial w)dx$, where $\partial w/\partial x$ is the slope of the panel along the x axis.

Similar to classical plate theory for homogeneous and isotropic materials (Timoshenko and Woinowsky-Krieger, 1959), and classical laminated plate theory (see above), first-order shear deformation theory assumes that plane sections of the core, originally perpendicular to the plane of the sandwich panel remain plane after deformation. According to this theory, however,

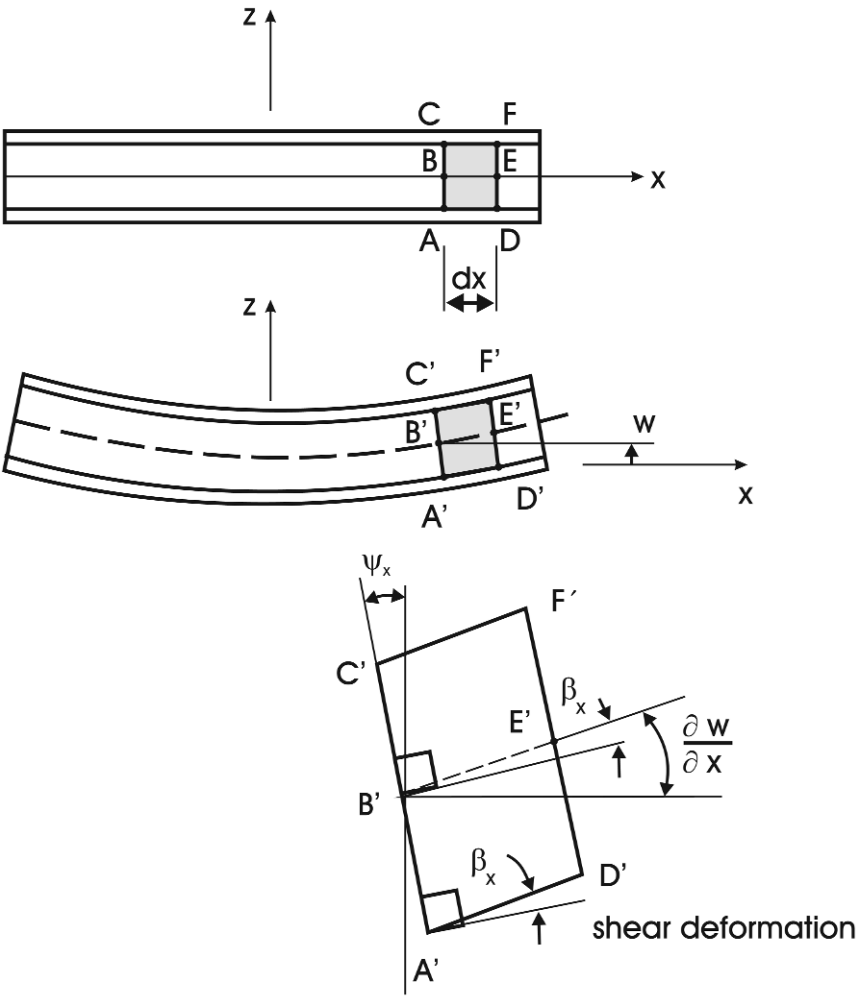

Figure 3.12 Deformation of core element in the x–z plane.

the cross-sections may not necessarily remain perpendicular to the deformed middle surface of the core, as shown in Figure 3.12. The slope of the middle surface, $\partial w/\partial x$ differs from the magnitude of the rotation of the cross-section, $|\psi_x|$, and the difference (β_x) constitutes the shear deformation. From Figure 3.12, it is recognized that

$$\beta_x = \frac{\partial w}{\partial x} - |\psi_x|, \tag{3.32}$$

where the rotation, ψ_x, as shown in Figure 3.12 is negative ($\psi_x < 0$) while the slope is shown positive. Hence, the shear strain is

$$\gamma_{xy} = \psi_x + \frac{\partial w}{\partial x}. \tag{3.33}$$

This analysis applies to all points at position x and hence implies that the shear strain is uniform through the thickness of the core. Similar considerations may be formulated for core sections perpendicular to the y axis.

The in-plane strains are obtained from Equations (3.2a, b and f) and (3.30)

$$\varepsilon_x = \varepsilon_x^0 + z\kappa_x, \tag{3.34a}$$

$$\varepsilon_y = \varepsilon_y^0 + z\kappa_x, \tag{3.34b}$$

$$\gamma_{xy} = \gamma_{xy}^0 + z\kappa_{xy}, \tag{3.34c}$$

where $[\varepsilon_x^0, \varepsilon_y^0, \gamma_{xy}^0]$ are the mid-core strains defined by

$$\varepsilon_x^0 = \frac{\partial u_0}{\partial x}, \tag{3.35a}$$

$$\varepsilon_y^0 = \frac{\partial v_0}{\partial y}, \tag{3.35b}$$

$$\gamma_{xy}^0 = \frac{\partial u_0}{\partial y} + \frac{\partial v_0}{\partial x} \tag{3.35c}$$

and the mid-core curvatures $[\kappa_x, \kappa_y, \kappa_{xy}]$ are

$$\kappa_x = \frac{\partial \psi_x}{\partial x}, \tag{3.36a}$$

$$\kappa_y = \frac{\partial \psi_y}{\partial y}, \tag{3.36b}$$

$$\kappa_{xy} = \frac{\partial \psi_x}{\partial y} + \frac{\partial \psi_y}{\partial x}. \tag{3.36c}$$

The out-of-plane shear strains, γ_{yz} and γ_{xz}, are defined in Equations (3.2d, e) which, combined with Equations (3.30), yield

$$\gamma_{xz} = \psi_x + \frac{\partial w}{\partial x}, \tag{3.37a}$$

$$\gamma_{yz} = \psi_y + \frac{\partial w}{\partial y}. \tag{3.37b}$$

The out-of-plane extensional strain in the core, ε_z, vanishes according to assumption (iv).

Labeling the bottom and top face sheets by (1) and (2), their in-plane strains become (Equations (3.36)),

Bottom

$$\varepsilon_x(1) = \varepsilon_x^0 - \frac{(h_c + h_1)}{2}\kappa_x, \tag{3.38a}$$

$$\varepsilon_y(1) = \varepsilon_y^0 - \frac{(h_c + h_1)}{2}\kappa_y, \tag{3.38b}$$

$$\gamma_{xy}(1) = \gamma_{xy}^0 - \frac{(h_c + h_1)}{2}\kappa_{xy}. \tag{3.38c}$$

Top

$$\varepsilon_x(2) = \varepsilon_x^0 + \frac{(h_c + h_2)}{2}\kappa_x, \tag{3.38d}$$

$$\varepsilon_y(2) = \varepsilon_y^0 + \frac{(h_c + h_2)}{2}\kappa_y, \tag{3.38e}$$

$$\gamma_{xy}(2) = \gamma_{xy}^0 + \frac{(h_c + h_2)}{2}\kappa_{xy}. \tag{3.38f}$$

The force and moment resultants for a sandwich element (Figure 3.13) are obtained by integrating the stresses over the element thickness,

$$(N_x, N_y, N_{xy}) = \int_{-(h_c/2+h_1)}^{-h_c/2} (\sigma_x(1), \sigma_y(1), \tau_{xy}(1))dz + \int_{h_c/2}^{h_c/2+h_2} (\sigma_x(2), \sigma_y(2), \tau_{xy}(2))dz, \tag{3.39a}$$

$$(M_x, M_y, M_{xy}) = \int_{-(h_c/2+h_1)}^{-h_c/2} (\sigma_x(1), \sigma_y(1), \tau_{xy}(1))zdz + \int_{h_c/2}^{h_c/2+h_2} (\sigma_x(2), \sigma_y(2), \tau_{xy}(2))zdz, \tag{3.39b}$$

$$(Q_x, Q_y) = \int_{-h_c/2}^{h_c/2} (\tau_{xz}, \tau_{yz})dz. \tag{3.39c}$$

Notice that the in-plane normal and in-plane shear stresses in the core are neglected by virtue of assumption (ii).

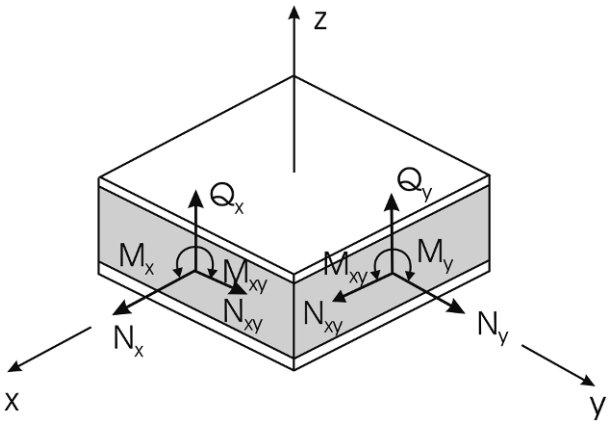

Figure 3.13 Force and moment resultants for a sandwich element.

The in-plane stresses in each ply (k) of the face sheets are given by Equation (3.15)

$$\begin{bmatrix} \sigma_x(i) \\ \sigma_y(i) \\ \tau_{xy}(i) \end{bmatrix}_k = \begin{bmatrix} \bar{Q}_{11} & \bar{Q}_{12} & \bar{Q}_{16} \\ \bar{Q}_{12} & \bar{Q}_{22} & \bar{Q}_{26} \\ \bar{Q}_{16} & \bar{Q}_{26} & \bar{Q}_{66} \end{bmatrix}_k \begin{bmatrix} \varepsilon_x(i) \\ \varepsilon_y(i) \\ \gamma_{xy}(i) \end{bmatrix}, \tag{3.40}$$

where k is the ply index (Figure 3.1) and $i = 1$ for the lower face, and $i = 2$ for the upper face. The matrix in Equation (3.40) is the transformed plane stress stiffness matrix as defined in Appendix A.

Substitution of the in-plane stresses given by Equations (3.40) into the expressions for the force and moment resultants (3.39a, b) yields

$$\begin{bmatrix} N_x \\ N_y \\ N_{xy} \end{bmatrix} = \begin{bmatrix} A_{11} & A_{12} & A_{16} \\ A_{12} & A_{22} & A_{26} \\ A_{16} & A_{26} & A_{66} \end{bmatrix} \begin{bmatrix} \varepsilon_x^0 \\ \varepsilon_y^0 \\ \gamma_{xy}^0 \end{bmatrix} + \begin{bmatrix} B_{11} & B_{12} & B_{16} \\ B_{12} & B_{22} & B_{26} \\ B_{16} & B_{26} & B_{66} \end{bmatrix} \begin{bmatrix} \kappa_x \\ \kappa_y \\ \kappa_{xy} \end{bmatrix}, \tag{3.41}$$

$$\begin{bmatrix} M_x \\ M_y \\ M_{xy} \end{bmatrix} = \begin{bmatrix} C_{11} & C_{12} & C_{16} \\ C_{12} & C_{22} & C_{26} \\ C_{16} & C_{26} & C_{66} \end{bmatrix} \begin{bmatrix} \varepsilon_x^0 \\ \varepsilon_y^0 \\ \gamma_{xy}^0 \end{bmatrix} + \begin{bmatrix} D_{11} & D_{12} & D_{16} \\ D_{12} & D_{22} & D_{26} \\ D_{16} & D_{26} & D_{66} \end{bmatrix} \begin{bmatrix} \kappa_x \\ \kappa_y \\ \kappa_{xy} \end{bmatrix}, \tag{3.42}$$

where

$$A_{ij} = A_{ij}(1) + A_{ij}(2), \tag{3.43a}$$

$$B_{ij} = \frac{(h_c + h_2)}{2} A_{ij}(2) - \frac{(h_c + h_1)}{2} A_{ij}(1), \tag{3.43b}$$

$$C_{ij} = C_{ij}(1) + C_{ij}(2), \tag{3.43c}$$

$$D_{ij} = \frac{(h_c + h_2)}{2} C_{ij}(2) - \frac{(h_c + h_1)}{2} C_{ij}(1), \tag{3.43d}$$

with

$$A_{ij}(1), C_{ij}(1) = \int_{-(h_c/2+h_1)}^{-h_c/2} \bar{Q}_{ij}(1, z)dz \quad \text{(bottom face)}, \tag{3.44a}$$

$$A_{ij}(2), C_{ij}(2) = \int_{h_c/2}^{h_c/2+h_2} \bar{Q}_{ij}(1, z)dz \quad \text{(top face)}. \tag{3.44b}$$

It may be shown that a symmetric sandwich plate, i.e., where the top and bottom faces are laid-up such that the mid-plane ($z = 0$) of the sandwich panel is a symmetry (mirror) plane; for example, the bottom face (#1) is a [0/90] laminate and the top face (#2) is a [90/0] laminate, fulfills the following equations:

$$A_{ij}(1) = A_{ij}(2), \tag{3.45a}$$

$$C_{ij}(1) = -C_{ij}(2). \tag{3.45b}$$

As a result, Equations (3.45) in (3.43) give

$$A_{ij} = 2A_{ij}(2), \tag{3.46a}$$

$$B_{ij} = 0 = C_{ij}, \tag{3.46b}$$

$$D_{ij} = (h_c + h_f)C_{ij}(2), \tag{3.46c}$$

where $h_f = h_1 = h_2$, is the face thickness.

Consequently, for such a panel the constitutive Equations (3.41) and (3.42) uncouple and become

$$\begin{bmatrix} N_x \\ N_y \\ N_{xy} \end{bmatrix} = \begin{bmatrix} A_{11} & A_{12} & A_{16} \\ A_{12} & A_{22} & A_{26} \\ A_{16} & A_{26} & A_{66} \end{bmatrix} \begin{bmatrix} \varepsilon_x^0 \\ \varepsilon_y^0 \\ \gamma_{xy}^0 \end{bmatrix}, \tag{3.47}$$

$$\begin{bmatrix} M_x \\ M_y \\ M_{xy} \end{bmatrix} = \begin{bmatrix} D_{11} & D_{12} & D_{16} \\ D_{12} & D_{22} & D_{26} \\ D_{16} & D_{26} & D_{66} \end{bmatrix} \begin{bmatrix} \kappa_x \\ \kappa_y \\ \kappa_{xy} \end{bmatrix}. \tag{3.48}$$

Another simplification of the analysis is obtained by treating the face sheets as homogeneous materials with average stiffnesses

$$\bar{Q}_{ij}(1) = A_{ij}(1)/h_1, \tag{3.49a}$$

$$\bar{Q}_{ij}(2) = A_{ij}(2)/h_2. \tag{3.49b}$$

For this case, the integrals in Equations (3.44) become

$$C_{ij}(1) = \frac{-A_{ij}(1)}{2}(h_c + h_1), \tag{3.50a}$$

$$C_{ij}(2) = \frac{A_{ij}(2)}{2}(h_c + h_2). \tag{3.50b}$$

Substitution in Equations (3.43) gives

$$A_{ij} = A_{ij}(1) + A_{ij}(2), \tag{3.51a}$$

$$B_{ij} = \frac{(h_c + h_2)}{2}A_{ij}(2) - \frac{(h_c + h_1)}{2}A_{ij}(1), \tag{3.51b}$$

$$C_{ij} = B_{ij}, \tag{3.51c}$$

$$D_{ij} = \left(\frac{h_c + h_1}{2}\right)^2 A_{ij}(2) + \left(\frac{h_c + h_2}{2}\right)^2 A_{ij}(2). \tag{3.51d}$$

For a symmetric sandwich with homogeneous faces: $A_{ij}(1) = A_{ij}(2) = \bar{Q}_{ij}(f)h_f$, and $h_1 = h_2 = h_f$, which leads to

$$A_{ij} = 2A_{ij}(2) = 2\bar{Q}_{ij}(f)h_f, \tag{3.52a}$$

$$B_{ij} = C_{ij} = 0, \tag{3.52b}$$

$$D_{ij} = 2\left(\frac{h_c + h_f}{2}\right)^2 \bar{Q}_{ij}(f)h_f. \tag{3.52c}$$

The expression for the flexural stiffness, Equation (3.52c), is the plate equivalent to the beam equation (1.8) for a sandwich beam with thin faces.

For calculation of the transverse shear resultants, Q_x and Q_y, defined in Equation (3.39c) and shown in Figure 3.13, the shear stresses in the core, τ_{xz} and τ_{yz}, are given in terms of the shear strains, γ_{xz} and γ_{yz} by

$$\tau_{xz} = G_{xz}\gamma_{xz}, \tag{3.53a}$$

$$\tau_{yz} = G_{yz}\gamma_{yz}, \tag{3.53b}$$

where G_{xz} and G_{yz} are the transverse shear moduli of the core.

In shear deformation theory for homogeneous plates, it is customary to use a correction factor (k), or correction factors (k_1 and k_2) for the transverse shear strains as introduced by Reissner (1945), Mindlin (1951), and Chow (1971), although a single factor is most commonly used for both transverse shear strains. The factor k is introduced as a multiplicative parameter in the constitutive relations between transverse shear forces and transverse shear strains (see, e.g., Whitney, 1987). The need for a correction factor in first-order theory for homogeneous plates originates from the fact that the transverse shear strains and shear stresses are uniform through the thickness instead of the classical parabolic shear stress distribution with zero shear stresses on the surfaces of the plate. The correction factor k is determined from exact solutions for the shear stresses at the center of the plate in terms of the transverse shear forces or from the total strain energy due to transverse shear forces (Whitney, 1987). Whitney (1972) determined two correction factors (k_1 and k_2) for the transverse shear strains in a sandwich panel by fitting the first-order shear results to an exact solution by Pagano (1970a). Most commonly, however, shear correction factors are not used for sandwich panels since the core shear stress indeed is fairly constant throughout the thickness of the core (see, e.g., Section 2.2). Furthermore, the faces are assumed free from shear stresses (assumption (i)). With no shear correction factor, integration of the (constant) shear stress given by Equations (3.37) into (3.53) over the core thickness (Equation (3.39c)) yields

$$Q_x = h_c G_{xz} \left(\psi_x + \frac{\partial w}{\partial x} \right), \tag{3.54a}$$

$$Q_y = h_c G_{yz} \left(\psi_y + \frac{\partial w}{\partial y} \right). \tag{3.54b}$$

3.2.1 Alternative Form of the Constitutive Equations for a Sandwich Plate Element

The force and moment resultants given by Equations (3.41) and (3.42) may be written in compressed form as

$$[N] = [N][\varepsilon^0] + [B][\kappa], \tag{3.55a}$$

$$[M] = [C][\varepsilon^0] + [D][\kappa], \tag{3.55b}$$

where $[N]$ and $[M]$ represent the 3×1 force and moment resultants, $[A]$, $[B]$, $[C]$ and $[D]$ are the 3×3 elastic stiffness matrices, and $[\varepsilon^0]$ and $[\kappa]$ are the

3×1 core mid-plane strains and curvatures, respectively. Equations (3.55) may also be written as

$$\begin{bmatrix} N \\ M \end{bmatrix} = \begin{bmatrix} A & B \\ C & D \end{bmatrix} \begin{bmatrix} \varepsilon^0 \\ \kappa \end{bmatrix}, \tag{3.56}$$

where the $ABCD$ matrix is of dimension 6×6.

Equations (3.56) are convenient when force and moment resultants are to be determined from known mid-core strains and curvatures. Often it is desirable to express the core mid-core strains and curvatures in terms of force and moment resultants, and this is achieved by inversion of the 6×6 $ABCD$ matrix in Equations (3.56)

$$\begin{bmatrix} \varepsilon^0 \\ \kappa \end{bmatrix} = \begin{bmatrix} a & b \\ c & d \end{bmatrix} \begin{bmatrix} N \\ M \end{bmatrix}, \tag{3.57}$$

where expressions for the 3×3 compliance matrices $[a]$, $[b]$, $[c]$ and $[d]$ in terms of $[A]$, $[B]$, $[C]$ and $[D]$ are provided in Appendix B.

3.2.2 Equilibrium Equations

The equilibrium equations for force and moment resultants are presented by Whitney (1987). These equations are

$$\frac{\partial N_x}{\partial x} + \frac{\partial N_{xy}}{\partial y} = 0, \tag{3.58a}$$

$$\frac{\partial N_{xy}}{\partial x} + \frac{\partial N_y}{\partial y} = 0, \tag{3.58b}$$

$$\frac{\partial M_x}{\partial x} + \frac{\partial M_{xy}}{\partial y} - Q_x = 0, \tag{3.58c}$$

$$\frac{\partial M_{xy}}{\partial x} + \frac{\partial M_y}{\partial y} - Q_y = 0, \tag{3.58d}$$

$$\frac{\partial Q_x}{\partial x} + \frac{\partial Q_y}{\partial y} + N_x \frac{\partial^2 w}{\partial x^2} + 2N_{xy} \frac{\partial^2 w}{\partial x \partial y} + N_y \frac{\partial^2 w}{\partial y^2} + q = 0, \tag{3.58e}$$

with

$$q = \sigma_z(h/2) - \sigma_z(-h/2), \tag{3.58f}$$

where h is the thickness of the sandwich plate.

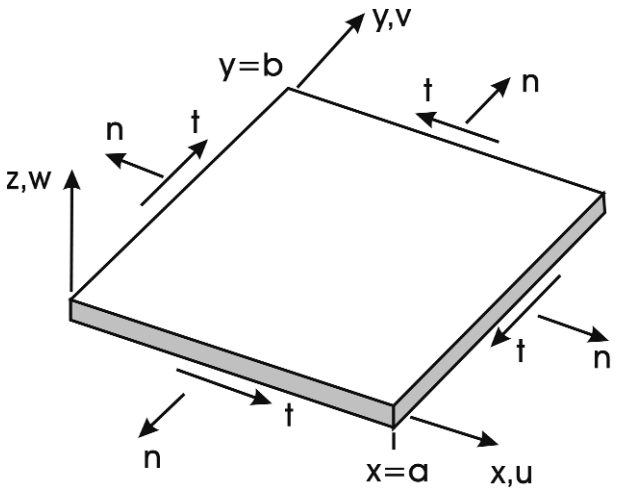

Figure 3.14 Definition of normal and tangential directions for a rectangular panel.

3.2.3 Boundary Conditions for a Rectangular Panel

We will consider a rectangular panel with the x and y coordinate axes parallel to the edges of the panel such as shown in Figure 3.14. The proper boundary conditions are necessary to guarantee achievement of a unique solution of the governing equations. Such conditions may be achieved by inspection of the problem which will reveal some of the more obvious boundary conditions. Other boundary conditions may be obtained by applying energy principles and calculus of variations (Whitney, 1987). Boundary conditions for rectangular plates refer to the normal and tangential in-plane directions as defined in Figure 3.14.

Boundary conditions specified for the present shear deformation theory requires specification of displacements, forces, and moments with respect to the normal and tangential directions of the panel (Figure 3.14). Five boundary conditions are generally required.

Simply-Supported

Figure 3.15 illustrates simply supported conditions for the edge $x = 0$, i.e., the deflection, w, is zero along the edge and at the same time, the edge can rotate freely with respect to a line along the edge ($x = 0$), i.e., $M_x = 0$ along this edge.

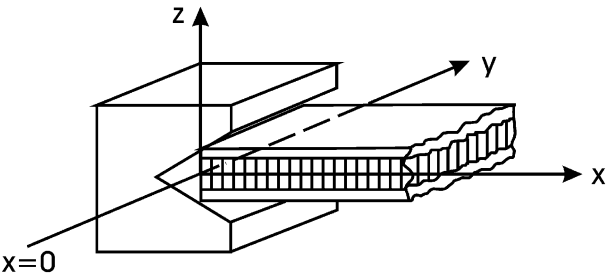

Figure 3.15 Illustration of simply-supported boundary conditions at $x = 0$.

Furthermore, the edge is assumed not to transfer normal and shear forces and prohibit rotations of the panel along the y axis, i.e., $N_x = N_{xy} = 0$, and the rotations $\psi_y = 0$ along this edge. In summary, we have

$$w(0, y) = M_x(0, y) = N_x(0, y) = N_{xy}(0, y) = \psi_y(0, y) = 0. \quad (3.59)$$

If all edges are simply supported, similar conditions apply for the edges $x = a$, $y = 0$, and $y = b$.

Hinged-Free Perpendicular to the Edge

If the edge, $x = 0$, is moment-free (hinged) and free to move in a direction normal to the edge (here along the x axis), the following conditions apply

$$N_x(0, y) = v_0(0, y) = M_x(0, y) = \psi_y(0, y) = w(0, y) = 0. \quad (3.60)$$

Hinged-Free Parallel to the Edge

If the edge, $x = 0$, is hinged and free to move tangentially, the following conditions apply:

$$u_0(0, y) = N_{xy}(0, y) = M_x(0, y) = \psi_y(0, y) = w(0, y) = 0. \quad (3.61)$$

Clamped

If the edge, $x = 0$, is clamped or "built-in", the deflection, w, along the edge is zero and the rotations, ψ_x and ψ_y, as well as mid-core displacements u_0 and v_0 (Equations (3.30)), are zero, i.e.

$$w(0, y) = \psi_x(0, y) = \psi_y(0, y) = u_0(0, y) = v_0(0, y) = 0. \quad (3.62)$$

Free Edge

If the edge, $x = 0$, is completely unconstrained, there are no resulting normal and shear forces in the plane, no bending and twisting moments, and no transverse shear force, i.e.,

$$N_x(0, y) = N_{xy}(0, y) = M_x(0, y) = M_{xy}(0, y) = Q_x(0, y) = 0. \quad (3.63)$$

3.3 Analysis of a Transversely Loaded Sandwich Plate

Sandwich panels are common structural elements in sandwich constructions such as boat hulls and containers. Analysis of flat sandwich panels of rectangular shape have been conducted by several investigators, e.g. Yen et al. (1951), Reissner (1948), Hoff (1950), and Riber (1997), and both linear small deflection analysis and geometrical nonlinear behavior have been addressed. In this section we will present analysis of the small deflection response of simply supported rectangular sandwich panels under transverse loading.

The strain-displacement relations for the core are those of Equations (3.30):

$$u = u_0 + z\psi_x, \quad (3.64a)$$

$$v = v_0 + z\psi_y, \quad (3.64b)$$

$$w = w_0. \quad (3.64c)$$

The face displacements are specified in Equations (3.31). The sandwich panel is assumed to be of symmetric construction and the face sheets are treated as homogeneous specially orthotropic materials. Hence, the constitutive relations for the force and moment resultants are given by (Equations (3.47) and (3.48))

$$\begin{bmatrix} N_x \\ N_y \\ N_{xy} \end{bmatrix} = \begin{bmatrix} A_{11} & A_{12} & 0 \\ A_{12} & A_{22} & A_{26} \\ 0 & 0 & A_{66} \end{bmatrix} \begin{bmatrix} \varepsilon_x^0 \\ \varepsilon_y^0 \\ \gamma_{xy}^0 \end{bmatrix}, \quad (3.65)$$

$$\begin{bmatrix} M_x \\ M_y \\ M_{xy} \end{bmatrix} = \begin{bmatrix} D_{11} & D_{12} & 0 \\ D_{12} & D_{22} & 0 \\ 0 & 0 & D_{66} \end{bmatrix} \begin{bmatrix} \kappa_x \\ \kappa_y \\ \kappa_{xy} \end{bmatrix}, \quad (3.66)$$

where, according to Equations (3.52),

$$A_{ij} = 2A_{ij}(f), \tag{3.67a}$$

$$D_{ij} = 2\left(\frac{h_c + h_f}{2}\right)^2 A_{ij}(f). \tag{3.67b}$$

For transverse shear loading, the constitutive equations (3.54) read

$$Q_x = h_c G_{xz}\left(\psi_x + \frac{\partial w}{\partial x}\right), \tag{3.68a}$$

$$Q_y = h_c G_{yz}\left(\psi_y + \frac{\partial w}{\partial y}\right). \tag{3.68b}$$

Substitution of the constitutive equations (3.65), (3.66) and (3.68) into the equilibrium equations (3.58) yields the following set of governing differential equations valid for symmetric sandwich panels with specially orthotropic or isotropic face sheets:

$$A_{11}\frac{\partial u_0}{\partial x^2} + (A_{12} + A_{66})\frac{\partial^2 v_0}{\partial x \partial y} + A_{66}\frac{\partial^2 u_0}{\partial y^2} = 0, \tag{3.69a}$$

$$A_{22}\frac{\partial^2 v_0}{\partial y^2} + (A_{12} + A_{66})\frac{\partial^2 u_0}{\partial x \partial y} + A_{66}\frac{\partial^2 v_0}{\partial x^2} = 0, \tag{3.69b}$$

$$D_{11}\frac{\partial^2 \psi_x}{\partial x^2} + (D_{12} + D_{66})\frac{\partial^2 \psi_y}{\partial x \partial y} + D_{66}\frac{\partial^2 \psi_x}{\partial y^2} - h_c G_{xz}\left(\psi_x + \frac{\partial w}{\partial x}\right) = 0, \tag{3.69c}$$

$$D_{22}\frac{\partial^2 \psi_y}{\partial y^2} + (D_{12} + D_{66})\frac{\partial^2 \psi_x}{\partial x \partial y} + D_{66}\frac{\partial^2 \psi_y}{\partial x^2} - h_c G_{yz}\left(\psi_y + \frac{\partial w}{\partial y}\right) = 0, \tag{3.69d}$$

$$h_c G_{xz}\left(\frac{\partial \psi_x}{\partial x} + \frac{\partial^2 w}{\partial x^2}\right) + H_c G_{yz}\left(\frac{\partial \psi_y}{\partial y} + \frac{\partial^2 w}{\partial y^2}\right) + q = 0. \tag{3.69e}$$

We will specifically apply these equations to a transversely loaded sandwich panel of planar dimension a and b with the edges hinged and unconstrained parallel to the edges, see Figure 3.16. Specifically, the conditions stipulated for the edge defined by $x = 0$ in Equation (3.61) apply to all edges.

The transverse loading is most commonly represented by a double Fourier series (see, e.g., Whitney, 1987)

$$q(x, y) = \sum_{m=1}^{\infty}\sum_{n=1}^{\infty} q_{mn} \sin\frac{m\pi x}{a} \sin\frac{n\pi y}{b}. \tag{3.70}$$

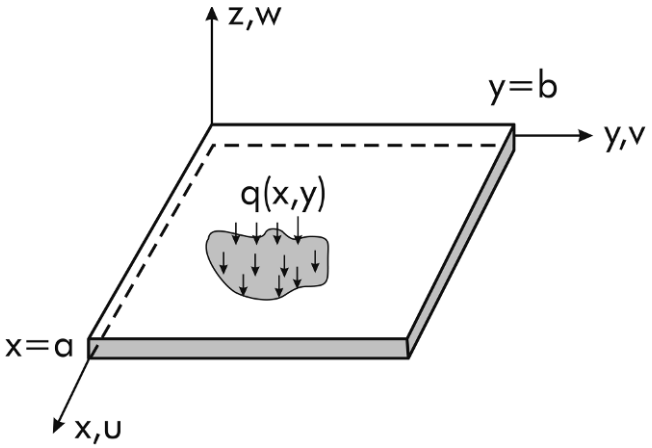

Figure 3.16 Rectangular sandwich panel under transverse loading.

The Fourier coefficients, q_{mn}, are determined from the actual load distribution, $q(x, y)$, using

$$q_{mn} = \frac{4}{ab}\int_0^a \int_0^b q(x, y) \sin\frac{m\pi x}{a} \sin\frac{n\pi y}{b} dxdy. \tag{3.71}$$

A common loading case studied is uniform pressure over the entire panel surface, $q = q_0 =$ constant. For this case, Equation (3.71) yields

$$q_{mn} = \frac{16q_0}{\pi^2 mn}, \quad m, n \text{ odd}, \tag{3.72a}$$

$$q_{mn} = 0, \quad m, n \text{ even}. \tag{3.72b}$$

Another important case is the rectangular area of uniform pressure shown in Figure 3.17. For this type of loading, Equation (3.71) yields

$$q_{mn} = \frac{16q_0}{\pi^2 mn} \sin\frac{m\pi\xi}{a} \sin\frac{m\pi\eta}{b} \sin\frac{m\pi c}{2a} \sin\frac{n\pi d}{2b}, \tag{3.73}$$

where ξ and η are the x and y coordinates of the center of the rectangle and c and d are the lengths of the rectangle along the x and y axes, see Figure 3.17.

A concentrated load, P, applied at $(x, y) = (\xi, \eta)$ may be represented by

$$q_{mn} = \frac{4P}{ab} \sin\frac{m\pi\xi}{a} \sin\frac{n\pi\eta}{b}. \tag{3.74}$$

By increasing the number of terms in the series, Equation (3.70), the exact solution will be approached asymptotically. The number of terms required

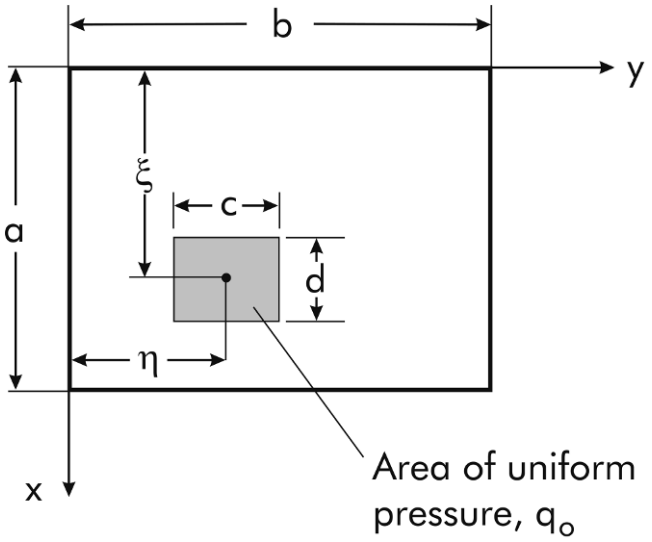

Figure 3.17 Rectangular panel loaded with uniform load over a rectangular region of the panel.

for a converged solution of the quantity of interest, i.e., deflection, strain or stress, must be examined for each case.

The analysis of a transversely loaded panels will here assume a simple one term case, i.e. $m = n = 1$, i.e. in Equation (3.70),

$$q(x, y) = q_0 \sin \frac{\pi x}{a} \sin \frac{\pi y}{b}. \tag{3.75}$$

Boundary conditions for rectangular panels are discussed in Section 3.2.3. In particular, the hinged-free tangential conditions defined in Equation (3.61) are assumed here. For the edges parallel to the y axis, $x = 0$ and a (Figure 3.16), the following conditions apply:

$$u_0 = 0, \tag{3.76a}$$

$$N_{xy} = A_{66}\left(\frac{\partial u_0}{\partial y} + \frac{\partial v_0}{\partial x}\right) = 0, \tag{3.76b}$$

$$w = 0, \tag{3.76c}$$

$$\psi_y = 0, \tag{3.76d}$$

$$M_x = D_{11}\frac{\partial \psi_x}{\partial x} + D_{12}\frac{\partial \psi_y}{\partial y} = 0. \tag{3.76e}$$

For the edges parallel to the x axis, $y = 0$ and b, the conditions are

$$v_0 = 0, \tag{3.77a}$$

$$N_{xy} = A_{66}\left(\frac{\partial u_0}{\partial y} + \frac{\partial v_0}{\partial x}\right) = 0, \tag{3.77b}$$

$$w = 0, \tag{3.77c}$$

$$\psi_x = 0, \tag{3.77d}$$

$$M_y = D_{12}\frac{\partial \psi_x}{\partial x} + D_{22}\frac{\partial \psi_y}{\partial y} = 0. \tag{3.77e}$$

A solution that satisfies the boundary conditions (3.76) and (3.77) consistent with the loading function, Equation (3.75), is given by

$$u_0 = A \sin\frac{\pi x}{a}\cos\frac{\pi y}{b}, \tag{3.78a}$$

$$v_0 = B \cos\frac{\pi x}{a}\sin\frac{\pi y}{b}, \tag{3.78b}$$

$$\psi_x = C \cos\frac{\pi x}{a}\sin\frac{\pi y}{b}, \tag{3.78c}$$

$$\psi_y = D \sin\frac{\pi x}{a}\cos\frac{\pi y}{b}, \tag{3.78d}$$

$$w = E \sin\frac{\pi x}{a}\sin\frac{\pi y}{b}. \tag{3.78e}$$

Substitution of Equations (3.78) into the governing equations (3.69) yields five equations conveniently expressed into the following matrix equation:

$$\begin{bmatrix} H_{11} & H_{12} & 0 & 0 & 0 \\ H_{12} & H_{22} & 0 & 0 & 0 \\ 0 & 0 & H_{33} & H_{34} & H_{35} \\ 0 & 0 & H_{34} & H_{44} & H_{45} \\ 0 & 0 & H_{35} & H_{45} & H_{55} \end{bmatrix} \begin{bmatrix} A \\ B \\ C \\ D \\ E \end{bmatrix} = \begin{bmatrix} 0 \\ 0 \\ 0 \\ 0 \\ q_0 \end{bmatrix}. \tag{3.79}$$

The elements H_{ij} of the symmetric 5×5 matrix are given by

$$H_{11} = \frac{A_{11}}{a^2} + \frac{A_{66}}{b^2}, \tag{3.80a}$$

$$H_{12} = \frac{A_{12} + A_{66}}{ab}, \tag{3.80b}$$

$$H_{22} = \frac{A_{22}}{b^2} + \frac{A_{66}}{a^2}, \tag{3.80c}$$

$$H_{33} = \frac{\pi^2 D_{11}}{a^2} + \frac{\pi^2 D_{66}}{b^2} + h_c G_{xz}, \tag{3.80d}$$

$$H_{34} = \frac{\pi(D_{12} + D_{66})}{ab}, \tag{3.80e}$$

$$H_{35} = \frac{\pi h_c G_{xz}}{a}, \tag{3.80f}$$

$$H_{44} = \frac{\pi^2 D_{22}}{b^2} + \frac{\pi^2 D_{66}}{a^2} + h_c G_{yz}, \tag{3.80g}$$

$$H_{45} = \frac{\pi h_c G_{yz}}{b}, \tag{3.80h}$$

$$H_{55} = \pi^2 h_c \left(\frac{G_{xz}}{a^2} + \frac{G_{yz}}{b^2} \right). \tag{3.80i}$$

Inversion of the H matrix, Equation (3.79), provides the constants A, B, C, D and E. The plate deflection is given by (Equation (3.78e))

$$w = E \sin \frac{\pi x}{a} \sin \frac{\pi y}{b}, \tag{3.81a}$$

with

$$E = h_{33} q_0, \tag{3.81b}$$

where

$$h_{33} = \frac{H_{33} H_{44} - H_{34}^2}{\det[H_{\text{sub}}]}. \tag{3.82}$$

$[H_{\text{sub}}]$ represents the following 3×3 submatrix defined by the last three rows and columns of the full matrix of Equation (3.79)

$$[H_{\text{sub}}] = \begin{bmatrix} H_{33} H_{34} H_{35} \\ H_{34} H_{44} H_{45} \\ H_{35} H_{45} H_{55} \end{bmatrix}. \tag{3.83}$$

The maximum deflection, $w_{\max}$, occurs at the panel center ($x = a/2$, $y = b/2$) and is given by

$$w_{\max} = E = h_{33} q_0. \tag{3.84}$$

A square ($a = b$) sandwich panel with unidirectional composite face sheets over an isotropic foam core is considered. The face sheets are assumed to consist of carbon/epoxy with the following mechanical properties:

$$E_1 = 125 \text{ GPa}, \quad E_2 = 5 \text{ GPa},$$

$$\nu_{12} = 0.25, \quad G_{12} = 2.5 \text{ GPa}.$$

The core considered is a H100 PVC foam with a shear modulus, $G = 60$ MPa. The thicknesses of the face sheets and core are $h_f = 2$ mm and $h_c = 16$ mm. Calculations of the deflection, $w_{\max}$, were conducted over a range of panel sizes. The side length, a, of the square panel was varied from 0.1 to 1.2 m. The bending stiffness elements D_{ij} were calculated from Equation (3.52c) which specifically applies to a symmetric sandwich with thin homogeneous face sheets.

Figure 3.18 displays the maximum deflection vs. the panel size, see the curve labeled SDPT (shear deformation plate theory). Also shown is the solution given by classical laminated plate theory (CLPT) (Whitney, 1987),

$$w_{\max} = \frac{q_0 a^4}{\pi^4 D(m = n = 1)}, \tag{3.85}$$

where $D(m = n = 1)$ is a bending stiffness term given by

$$D(m = n = 1) = D_{11} + 2(D_{12} + 2D_{66}) + D_{22}. \tag{3.86}$$

As discussed earlier, the CLPT formulation does not accommodate interlaminar shear deformation. Figure 3.18 shows that the CLPT results provide a lower bound to the deflection of the plate.

Figure 3.18 shows that the deflection of small plates with a thick core are quite substantially influenced by transverse shear deformation, while the deflection of larger panels is less affected by this mode of deformation and may be analyzed using CLPT.

3.4 Analysis of Sandwich Plate Twist Test

Tsai (1965) developed a plate twist test to determine the engineering elastic constants of orthotropic plates. The test utilized a square panel loaded at one corner and supported at the other corners. The panel response was analyzed using classical orthotropic plate theory (Lekhnitskii, 1968). By twisting a 0° panel and loading beams cut from the panel in bending, Tsai (1965) was able to determine all five elastic compliance constraints. Mure (1986) developed a two-point loading configuration of the plate twist test in order to determine the twisting stiffness (D_{66}) of corrugated core cardboard panels. Vinson

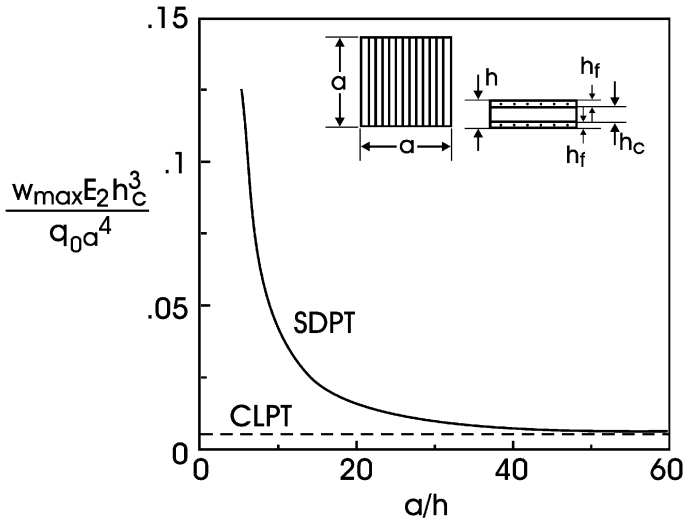

Figure 3.18 Maximum deflection of a square sandwich plate under transverse pressure load. CLPT and SDPT refer to classical laminated plate theory and shear deformation plate theory.

(1999) examined the test principle analytically in an effort to determine the in-plane shear strength of the face sheets, face/core adhesive or core, whatever constituent was the weakest. The plate twist test is also used to measure the in-plane shear modulus of plywood panels according to ASTM Standard D3044 (2000).

3.4.1 Classical Laminated Plate Theory Analysis

Figure 3.19 shows the two-point twist loading of a sandwich plate considered here. In this configuration, two diagonally opposite corners are loaded downwards by concentrated forces of magnitude $P/2$, while the other two corners are supported.

The sandwich plate is assumed to consist of identical isotropic or specially orthotropic faces. According to CLPT, the slopes of the middle surface are assumed to coincide (in magnitude) with the rotations of the cross-sections. Notice that this theory neglects transverse shear deformation. The following expressions for the plate curvatures defined in Equations (3.12) apply:

$$\kappa_x = -\frac{\partial^2 w}{\partial x^2}, \tag{3.87a}$$

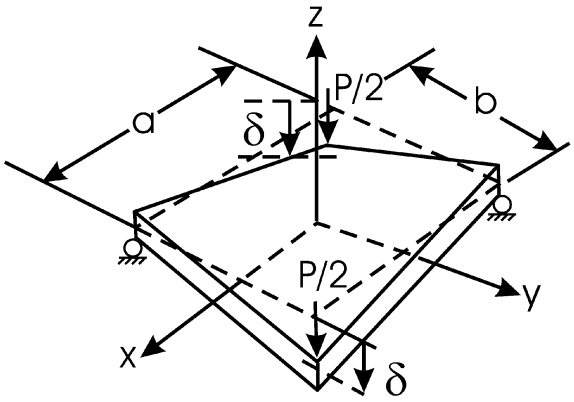

Figure 3.19 Illustration of loading and support conditions for the two-point sandwich plate twist test.

$$\kappa_y = -\frac{\partial^2 w}{\partial y^2}, \tag{3.87b}$$

$$\kappa_{xy} = -2\frac{\partial^2 w}{\partial y \partial x}. \tag{3.87c}$$

For a symmetric sandwich consisting of isotropic or specially orthotropic homogeneous face sheets, the pure twisting response is expressed by Equation (3.19)

$$M_{xy} = D_{66}\kappa_{xy}, \tag{3.88}$$

where the twisting stiffnesses, D_{66}, is given by Equation (3.20c) applied to a symmetric sandwich

$$D_{66} = (G_{12})_f h_f \left(\frac{2h_f^2}{3} + \frac{2h_c^2}{2} + h_f h_c\right) + \frac{(G_{12})_c h_c^3}{12}. \tag{3.89}$$

where $(G_{12})_f$ and $(G_{12})_c$ are the in-plane shear moduli of the face and core and h_f and h_c are the face and core thicknesses.

The twist loading shown in Figure 3.19 produces a twisting moment given by Timoshenko and Woinowsky-Krieger (1959),

$$M_{xy} = P/4. \tag{3.90}$$

A combination of Equations (3.88) and (3.90) yields

$$\kappa_{xy} = -2\frac{\partial^2 w}{\partial x \partial y} = \frac{P}{4D_{66}}. \tag{3.91}$$

The solution for the plate deflection representing a state of pure uniform twist curvature is, according to Lekhnitskii (1968), a second-order polynomial in x and y

$$w(x, y) = c_0 + c_1 x + c_2 y + c_3 xy. \tag{3.92}$$

The boundary conditions for the panel are (Figure 3.19),

$$w(a/2, -b/2) = w(-a/2, b/2) = 0, \tag{3.93a}$$

$$\frac{\partial w}{\partial x}(0, 0) = \frac{\partial w}{\partial y}(0, 0) = 0. \tag{3.93b}$$

Equations (3.91)–(3.93) yield

$$c_0 = \frac{ab}{4} c_5, \tag{3.94a}$$

$$c_1 = c_2 = 0, \tag{3.94b}$$

$$c_3 = \frac{-P}{8D_{66}}. \tag{3.94c}$$

Hence, the panel deflection becomes

$$w(x, y) = \frac{-P}{8D_{66}} \left(\frac{ab}{4} + xy \right). \tag{3.95}$$

The deflection of the loaded corners is given by $\delta = |w(a/2, b/2)|$. Equation (3.95) yields

$$\delta = \frac{Pab}{16D_{66}}. \tag{3.96}$$

The plate compliance is given by $C = \delta/P$. Hence,

$$C = \frac{ab}{16D_{66}}. \tag{3.97}$$

Measuring the compliance of the twisted plate should thus provide a means for determination of the twist stiffness D_{66}. It is noted that the only material parameters entering the expression for D_{66}, Equation (3.89), are the in-plane shear moduli for the faces and the core, $(G_{12})_f$ and $(G_{12})_c$. In most cases, the contribution to D_{66} from the core (the last term in Equation (3.89)) can be neglected because soft sandwich cores typically have $(G_{12})_c \ll (G_{12})_f$. For such a case, the twist test should provide a means to determine the in-plane shear modulus of the face sheets. As will be discussed in the next section, however, low modulus cores are susceptible to transverse shear deformation which will elevate the plate compliance.

3.4.2 Finite Element Analysis

It was pointed out that the compliance expression, Equation (3.97), does not include contributions due to transverse shear deformation. It is well known that shear deformation may influence the response of sandwich panels quite significantly, see Section 3.3. Furthermore, application of localized load to a sandwich panel is known to cause indentation deformation (Frostig et al., 1992; Thomsen, 1977). In order to further analyze, a sandwich panel under twist loading, finite element analysis was conducted by Aviles et al. (2009). A sandwich panel with a 25 mm thick foam core and 1 mm thick aluminum faces ($E = 70$ GPa, $\nu = 0.3$) was examined. The in-plane panel dimensions were 30.5×30.5 (cm). To reduce indentation deformation at load introduction and support points, square 10×10 (mm) areas were introduced at the contact regions at the corners, where the vertical displacement of the nodes was constrained to be uniform. Since sandwich panels are prone to transverse shear deformation in the core, a range of core shear moduli from 11.5 to 758 MPa was examined. The face sheets and core were modeled using the finite element code ANSYS (2006). All panels utilized the same mesh consisting of 3D eight-noded solid brick elements (SOLID 45).

Figure 3.20 presents the compliance of the sandwich panels calculated from FEA and CLPT vs. core-to-face shear modulus ratio (G_c/G_f). The compliance predicted by CLPT is fairly constant, since D_{66} is very little influenced by variations in G_c. The compliance predicted by FEA, on the other hand, decreases rapidly with increased core stiffness, until a plateau region is reached which coincides with the CLPT prediction. Convergence occurs for modulus ratios, $G_c/G_f > 14$. The large compliance for core materials with small core shear modulus is attributed to transverse shear deformation of the core (Aviles et al., 2009).

The results show that the compliance is extremely sensitive to changes in core shear modulus, G_c, when G_c is below about 100 MPa. Notice that several commercial PVC cores have shear modulus in this range (Table 1.3). Further, CLPT provides a very low estimate of the compliance unless the core is stiff. Thus, in general, the plate twist test is not a viable alternative to direct shear testing of the face sheets (Chapter 2). Further information on this test is provided in Aviles et al. (2009) and in Section 3.5.2.

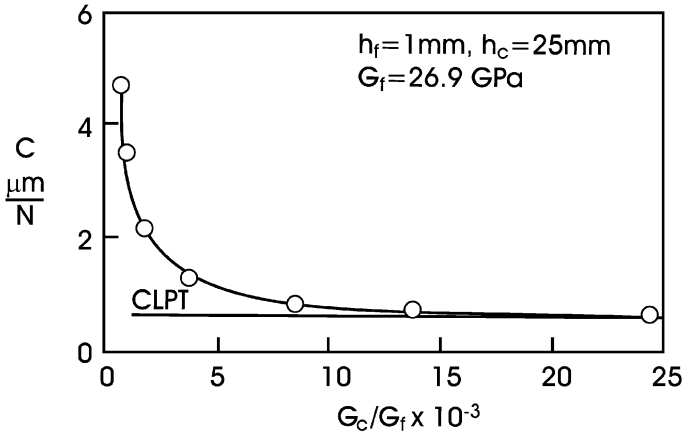

Figure 3.20 Compliance vs. core-to-face shear modulus ratio (G_c/G_f) for a 30.5 × 30.5 (cm) sandwich panel. $G_f = 26.9$ GPa.

3.5 Testing of Sandwich Panels

3.5.1 Pressure Loading of a Sandwich Plate

Testing of sandwich panels under distributed loading has been conducted by several investigators. The test is quite complex since it involves application of pressure over a quite large area in a controlled manner, while the edge conditions of the panel should be representative for those assumed in the analysis. Most reported test set-ups involve a pressurized water-filled rubber bladder to distribute the load over the panel surface in a uniform and controlled manner. The pressure in the bladder is controlled in order to achieve an accurate measure of the transverse load intensity, $q(x, y)$. Such an approach has been pursued by Rothschild et al. (1992), Bau-Madsen et al. (1992), Wennhage and Zenkert (1998), and Hayman et al. (1998).

Wennhage and Zenkert (1998) designed a test frame that was fitted in a large compression testing machine for testing of 0.85 × 0.85 (m) sandwich panels with a 25 mm thick H100 PVC foam core and 1 mm thick aluminum alloy faces ($E = 70$ GPa). The core mechanical properties are listed in Table 3.2. The faces were bonded to the core using a polyurethane adhesive. The panels were instrumented with four "shear plugs" consisting of 3 cm diameter cylindrical plugs of H100 core with a properly calibrated strain gage mounted at 45° to the cylinder axis (Moyer et al., 1992). The upper face of

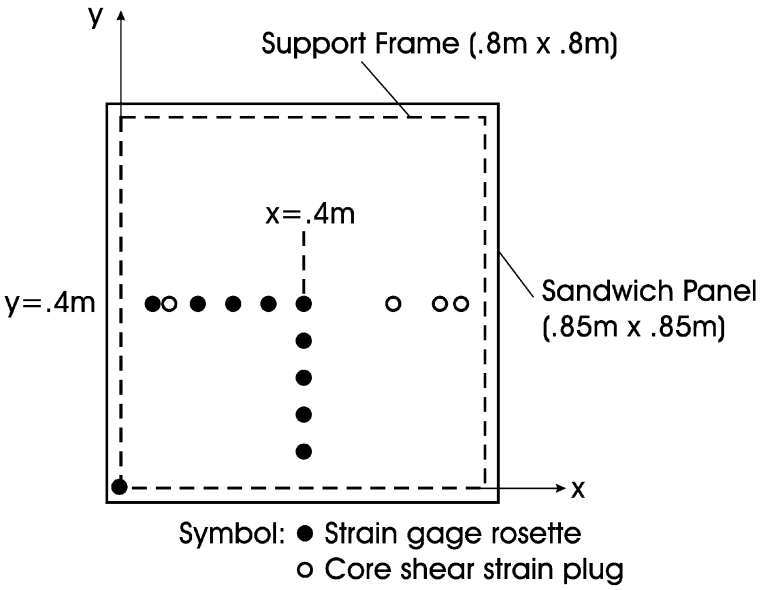

Figure 3.21 Location of surface mounted strain gages on sandwich panel (open circles) and core shear plugs (filled circles). The dotted line indicates line of support.

Table 3.1 Mechanical properties for H100 PVC foam core.

Shear modulus	Shear yield strength	Compressive strength
G	τ_y	σ_c
38 MPa	1.4 MPa	1.7 MPa

the sandwich panel was instrumented with ten 0°/90° strain gage rosettes, see the outline in Figure 3.21.

Notice that all strain gages, except for the one in the left corner, where the support lines intersect, were placed along the horizontal and vertical center lines representing symmetries of the panel. Figure 3.22 illustrates schematically the compression test procedure using the bladder system.

The testing rig consists of an upper frame made from rigid steel I beams with semi-circular rods of 20 mm diameter bolted to the lower surface of the I beams, Figure 3.22. The lower frame was made from rigid steel C beams. The primary purpose of the lower frame was to constrain the in-plane expansion of the rubber bladder. The rubber bladder was made from 2 mm thick EPDM rubber. It was filled with water and sealed prior to testing. The rounded steel bars are intended to provide simply supported edge boundary

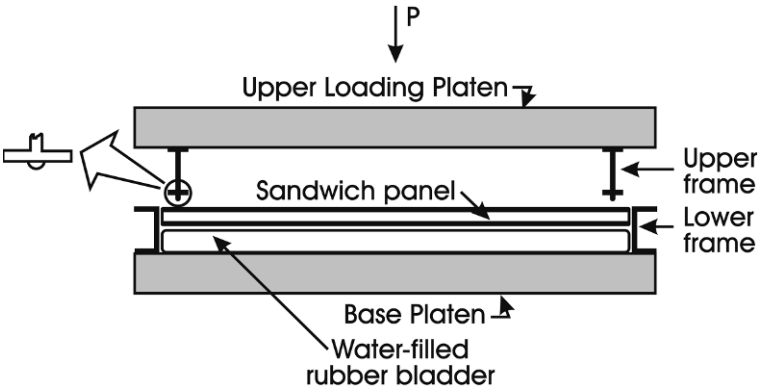

Figure 3.22 Principle of pressure loading of sandwich panel. Cross-sectional view in the x–z plane.

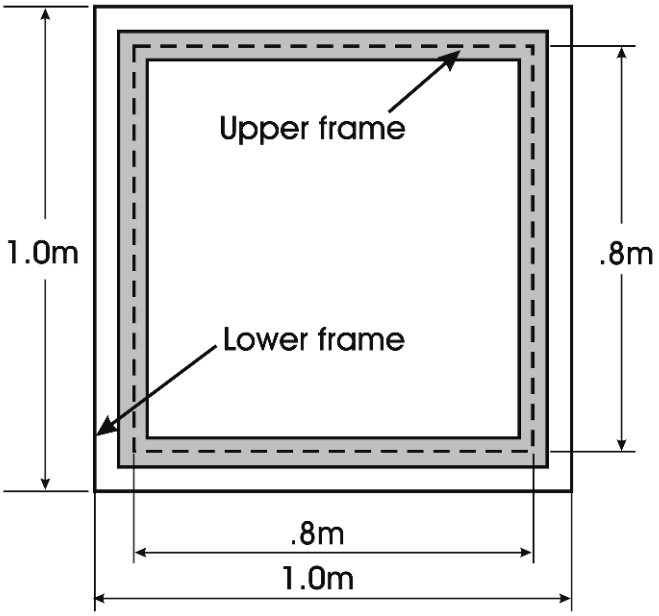

Figure 3.23 Top view of test panel and support structure.

conditions (Equation (3.59)) along the periphery of the panel, see the top view of the panel and the upper and lower frames shown in Figure 3.23.

In addition to the strain gage instrumentation (Figure 3.21), six displacement gages were attached to the upper loading platen of the test frame to measure the out-of-plane deflection of the panel along the symmetry lines

($x = 0.4$ and $y = 0.4$ m, Figure 3.21). The applied pressure loading was selected to maintain linear-elastic stress-strain behavior of all the constituents with a maximum stress less than or equal to 60% of the corresponding yield stress.

Test Results

The compressive load was increased to a maximum value of 50 kN, corresponding to a distributed pressure of 78 kPa over the 0.8×0.8 (m) test area. Such a pressure is not expected to cause compressive yielding of the H100 PVC foam core, see the material properties listed in Table 3.2.

It was found that the panel initially deviated somewhat from the ideal flat shape, i.e. it was slightly warped. All out-of-plane displacements readings were therefore corrected for deviation from flatness by subtracting the initial displacements from the actual readings. Upon further loading, the panels made full contact with the upper support fixture (Figure 3.22). Figure 3.24 shows experimental displacement data collected along symmetry lines ($x = 0.4$ and $y = 0.4$ m, Figure 3.21). Figure 3.24 also shows prediction of deflections from first-order sandwich plate analysis, see Section 3.5, using the loading function given by Equations (3.72) and simply supported boundary conditions (Equation (3.59)).

The experimental data reveal approximate symmetry with respect to the x and y directions, and there is good agreement between prediction and experimental data. Figure 3.25 shows the core shear stress results determined from the "shear plugs" embedded in the core. The shear stress is calculated from the measured shear strains using

$$\tau_{xz} = G_c \gamma_{xz}. \tag{3.98}$$

The predictions using sandwich plate theory analysis are overall in good agreement with the experimental data.

3.5.2 Plate Twist Testing

A test fixture for twist testing of sandwich panels was designed to represent the two-point configuration sketched in Figure 3.19. In this test configuration, two opposite corners are supported and two opposite corners are loaded. The fixture was designed for square panels with size up to about

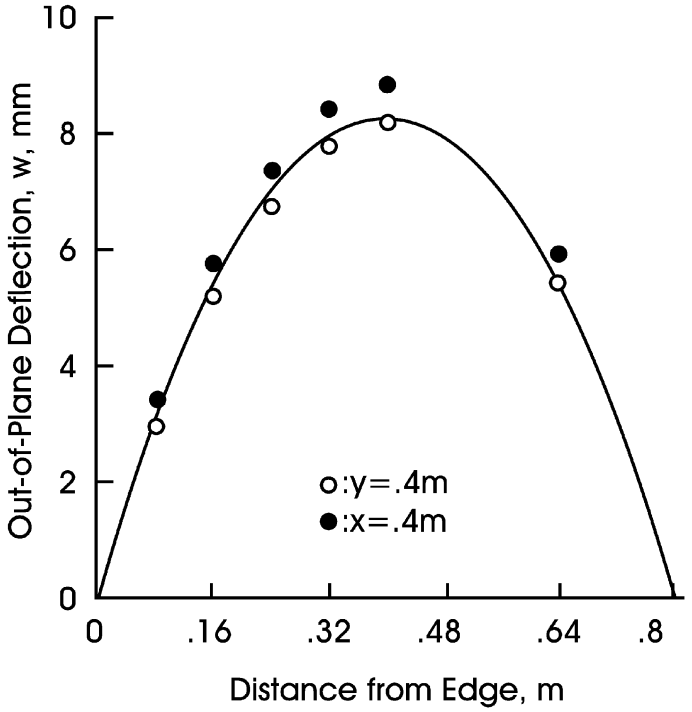

Figure 3.24 Measured and predicted plate deflections along symmetry lines ($x = 0.4$ m, $y = 0.4$ m).

30 × 30 (cm). Figure 3.26 shows a photograph of the test fixture with a slightly loaded sandwich panel. The fixture consists of a 30.5 × 30.5 × 1.28 (cm) aluminum plate bolted to the base of the test frame. To introduce load, a 46.5 cm long steel bar of cross-section 2.54 × 3.56 (cm) was attached to the load cell in the moving cross-head of the test machine. To allow testing of different size panels, multiple holes for attachment of support and loading pins were drilled in the bottom aluminum plate and in the steel bar, the outermost at a distance of 40.5 cm. The diagonally aligned holes in the aluminum base plate and longitudinal holes in the steel bar were spaced at increments of 1.27 cm. For loading and support of the panel at the desired points, steel pins of 9.5 mm diameter with hemispherical ends were inserted in the appropriate holes in the bottom plate and loading bar. The radius of the loading and support pin surfaces in contact with the panel was 4.75 mm.

A total of five square 30.5 × 30.5 (cm) (nominal dimensions) sandwich panels were prepared using aluminum face sheets and H80, H100, and H200 PVC foam cores. Panel dimensions and thicknesses of the constituents pan-

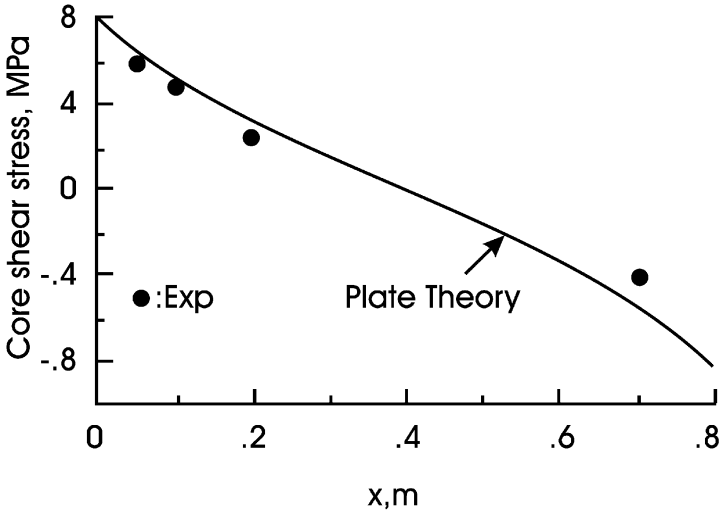

Figure 3.25 Core shear stress along symmetry section of the panel ($y = 0.4$ m).

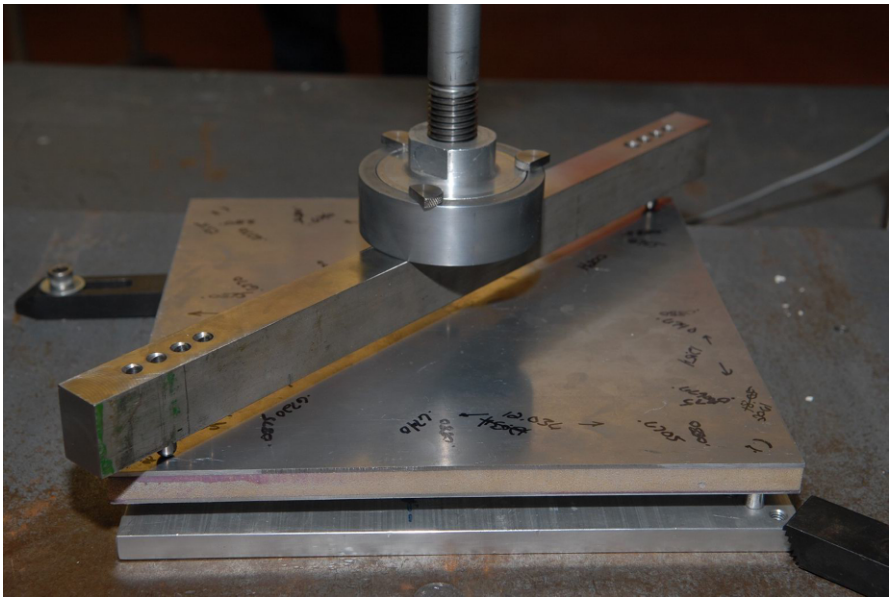

Figure 3.26 Sandwich plate twist test fixture.

els are listed in Table 3.3. The face sheets were nominally 1.5 and 2.25 mm thick labeled "thin" and "thick". The nominal core thickness was 12.7 mm. Table 3.2 lists the twisting stiffness, D_{66}, for each panel calculated from CLPT (Equation (3.89)) based on nominal face and core thicknesses.

Table 3.2 Dimensions and twist stiffness (D_{66}) of sandwich panels.

Panel	Core	h_f (mm)	h_c (mm)	h (mm)	a (cm)	D_{66} (kNm)
H80/Thin	H80	1.50	12.5	16.4	30.6	4.09
H100/Thick1	H100	2.26	12.8	17.6	30.6	6.90
H100/Thick2	H100	2.25	12.5	15.6	30.6	7.00
H200/Thin	H200	1.50	12.5	17.1	30.2	4.10
H200/Thick	H200	2.24	12.4	17.4	30.6	6.83

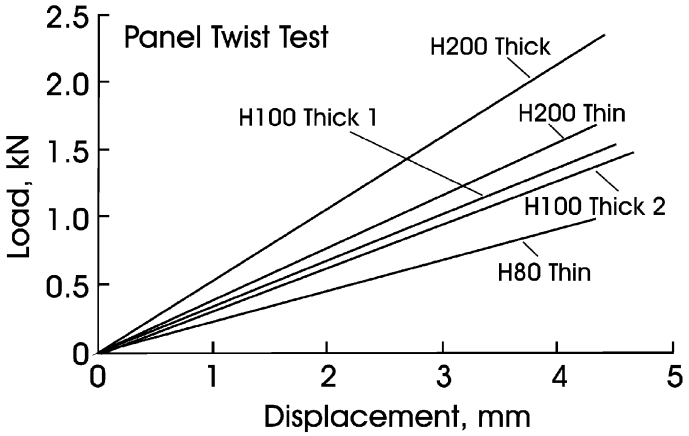

Figure 3.27 Load vs. deflection graphs for sandwich test panels.

Prior to testing of the sandwich panels, the machine/fixture compliance was determined by loading the fixture without a sandwich panel and measuring load and displacement. For testing a sandwich panel, the panel was inserted in the fixture, and adjusted so that the edges were aligned with the edges of the base plate, with the same amount of overhang at each edge. The deflection of the panel was measured using the cross-head displacement. The loading area was 27 × 27 (cm) in all tests. This corresponds to a nominal overhang length of about 1.75 cm. During testing of a sandwich panel, the first loading cycle revealed a stiffening nonlinear response at small loads. This was the result of local indentation deformation at load introduction and support locations, and slack in the fixture. Prior to the actual panel test, each panel was loaded to the maximum, and unloaded to about 500 N. This loading-unloading cycle was repeated a number of times until the loading and unloading load vs. displacement curves virtually coincided.

Figure 3.27 shows the experimental load vs. displacement curves for all the test panels (Table 3.3). Over the range of load levels from 0–2 kN, the

Table 3.3 Measured (Exp.), and CLPT and FEA predicted compliance values of sandwich panels.

Panel	C (μm/N)		
	Exp.	CLPT	FEA
H80/Thin	4.26	1.42	2.96
H100/Thick	3.01	0.85	1.91
H200/Thin	2.51	1.42	1.75
H200/Thick	1.82	0.85	1.27

response is linear and the loading and unloading curves virtually coincide. As expected, increased core density and face thickness result in a stiffer response.

After completion of the twist testing, the compliance of each specimen was determined from the load-displacement curves shown in Figure 3.27. Finite element analysis (FEA) of the actual test panels was conducted as explained in Section 3.4.2. The FEA was based on the nominal plate dimensions and an overhang of 15 mm. In all cases square 10 × 10 (mm) constrained areas were used at the load introduction and support regions.

Table 3.3 summarizes compliance values determined experimentally (Exp.) (corrected for machine compliance) and compliance values calculated from CLPT and FEA. The results in Table 3.3 reveal that CLPT substantially underestimates the compliance of the tested panels. The experimental results confirm the earlier assessment that CLPT is not accurate for analyzing the sandwich plate twist test, at least not for the sandwich panels considered here. The finite element predictions are much more close to the measured values, although the measured compliance values exceed the FEA predictions. The difference between FEA predictions and measured compliance value is attributed to more excessive indentation at load introduction and support points than accounted for in the finite element analysis.